

Applying ground gas and gas flux monitoring techniques to low-enthalpy, shallow geothermal energy exploration

Douglas Smith

British Geological Survey

Environmental Science Centre

Nicker Hill

Keyworth

Nottingham

NG12 5GG

Tel: 0782 1274437

Email: dosmi@bgs.ac.uk

Applying ground gas and gas flux monitoring techniques to low-enthalpy, shallow geothermal energy exploration

Douglas Smith^{a1}, Helen Taylor-Curran^a, Andrew Barkwith^a, Bob Lister^a, Karen Kirk^a, Sarah Hannis^b, Kirsty Shorter^b and Kyle Walker-Verkuil^b

1

2 **Abstract**

3

4 Ground gas and gas flux testing has been undertaken in a variety of situations including
5 volcanic and geothermal activity, landfill and carbon storage monitoring. However, there are
6 no documented studies of its application to shallow geothermal investigations, particularly
7 where the water in disused mines will be used as the conduit for heat and the overlying
8 ground has a complex industrial heritage. Background ground gas and gas flux
9 measurements from three separate campaigns at a mine water heat research site in
10 Glasgow, UK did not reveal any concerns regarding mine gas or other potentially harmful
11 gases from previous land uses. The detected CO₂ was found to be predominantly of
12 biological origin and reflected the expected quantities based upon land use, seasonal and
13 weather fluctuations and was consistent with other UK sites. One location is recommended
14 for further investigation due to higher-than-expected nitrogen and lower oxygen
15 measurements. Some hydrogen gas was detected, albeit well below explosive limits, which
16 may be present as a result of past industrial site uses, highlighting the need for more
17 investigation into the presence of hydrogen at ex-industrial sites. Apart from this there was
18 very little evidence of the industrial site history in the gas characterisation.

19

20 A process-based analysis, based upon the stoichiometric relationship of CO₂, CH₄, O₂ and N₂,
21 was applied to the results. This complemented, but was not a substitute for, the background
22 survey. There were limitations with the process-based approach when there was not a clear
23 anomalous CO₂ signal or where potentially more than one process was occurring
24 simultaneously.

25

^a British Geological Survey, Keyworth

^b British Geological Survey, Lyell Centre, Edinburgh

¹ Corresponding author

26 **Keywords (max 6)**

27

28 Shallow geothermal energy, mine gas, industrial site, background gas survey , process-based

29 analysis

30 1 Introduction

31

32 Measuring ground gas and gas flux at the surface or in the near-surface environment can be
33 a requirement, or simply responsible management, for subsurface energy or disposal
34 activities. It has been used in a variety of situations, such as detection of volcanic and
35 geothermal activity, monitoring landfill sites and for the investigation of the impacts related
36 to shale gas extraction (Cardellini et al., 2003; Zhang et al., 2017; Li et al., 2020 and Ward et
37 al., 2019). It has also been extensively considered and employed in monitoring the effects of
38 carbon capture and storage (CCS) (Beaubien et al., 2013; Carman et al., 2014; Pearce et al.,
39 2014; Beaubien et al., 2015; Jenkins et al., 2015; Jones et al., 2015 and Tarakki et al., 2018).
40 However, there is no record of it being applied to shallow geothermal energy production,
41 particularly where the water in disused mine workings provide the conduit for the heat
42 source; an immature but emerging technology in the UK (Athresh et al., 2015; Banks et al.,
43 2017; Farr et al., 2020; Coal Authority, 2021). This paper analyses the efficacy of ground gas
44 and gas flux measurements in determining the ground gas landscape and establishing
45 whether there are any pre-existing issues, such as the lensing or escape of mine gases, as a
46 result of the complex industrial history at the UK Geoenergy Observatory in Glasgow UK
47 ('Glasgow Observatory'); circumstances that are likely to recur if other mine workings are to
48 be utilised in this fashion.

49

50 The major gases associated with mine workings are methane (CH₄) and carbon dioxide (CO₂)
51 which, as well as being significant greenhouse gases, can accumulate to create asphyxiation
52 hazards, change the chemistry of ground water, affect biological processes, or explode
53 (Pearce et al., 2014; Jones et al., 2015; Blackford et al., 2014 and Appleton, 2011). Methane
54 that is adsorbed to the surface of coal is released when a coal seam is decompressed. In
55 mines the mix of methane with other gases, known as firedamp, can be explosive and has
56 resulted in a number of incidents. However, where present in sufficient quantities, coalbed
57 methane (CBM) can be recovered from coal seams and disused mines and used as an
58 additional source of hydrocarbons such as in USA, Australia, China and India (Jones et al.,
59 2004; Moore, 2012 and DECC, 2013). Jones et al. (2004) estimate that the coal in central
60 Glasgow has a methane content of 4.9 m³ t⁻¹, however, they note that this area had been
61 extensively mined so the potential for viable CBM is low. Flooding in the mines will also

62 prevent the desorption reducing the prevalence of free CH₄ gas (Jones et al., 2004). In
63 addition, the coal workings utilised for the Observatory are not sufficiently deep for CBM to
64 be feasible. Nonetheless, other potentially harmful trace gases associated with the mining
65 industry and other industrial uses, such as hydrogen sulphide (H₂S) and hydrogen (H₂), may
66 also be present (Young and Lawrence, 2001; Wilson et al., 2010). It is therefore important to
67 monitor for the presence of these gases throughout the development of the Observatory,
68 and of minewater geothermal activities more broadly.

69

70 1.1 Use of gas surveys in geo-energy projects

71

72 To understand gas in the near-surface environment, it is helpful to measure a number of
73 related parameters: firstly, ground gas concentrations, at a depth (c.70-100 cm below
74 ground level) that minimises or eliminates interference from the atmosphere. These
75 measurements correspond directly to concepts of 'soil gas' or 'near surface soil gas'
76 discussed elsewhere in the literature (for example, Ball et al., 1992; Beaubien et al., 2013);
77 secondly, gas flux measurements between soil and the lower atmosphere, a negative flux
78 indicates migration from the atmosphere into the soil; finally, if possible, measurement of
79 gas concentrations in the lower atmosphere, near to the ground surface.

80

81 These measurements are used, along with others, such as downhole, groundwater, soil and
82 surface water chemistry and seismic measurements, to construct an overall environmental
83 baseline that provides a picture of the typical conditions at a particular site (Pearce et al.,
84 2014). Within this comprehensive assessment, investigation of the normal gas environment
85 defines the site-specific geo-bio-chemical landscape, indicating the source of gas,
86 distinguishing gases produced by biological and chemical processes in soils and artificial
87 ground deposits and determining useful indicators of uncharacteristic behaviour (Beaubien,
88 2013; Jones et al., 2015 and Tarakki et al., 2018). This is often referred to as a 'baseline' or
89 'background' study and these terms are occasionally used interchangeably (e.g. Beaubien et
90 al., 2015). However, baseline implies a fixed level of environmental noise, which has allowed
91 this approach to be criticised as circumstances, such as climate change, will affect baseline
92 measurements throughout the life of a project (Dixon and Romanak, 2015). We believe the
93 term 'background' allows for such environmental fluctuations and is generally preferred in

94 relation to the activities described by this paper, however, the term baseline will still be
95 used when referring to other studies that define their inquiries as such.

96

97 Gas conditions fluctuate daily and seasonally and may also alter with changes in climate
98 (Beaubien et al., 2013; Dixon and Romanak, 2015). To capture the range of these cycles,
99 measurements are ideally taken through a combination of multiple discrete surveys,
100 preferably reflecting seasonal fluctuations, and continuous monitoring which allows diurnal
101 and seasonal patterns in gas to be accounted for. One of the most comprehensive baseline
102 studies was conducted at the Weyburn oil field, Saskatchewan, Canada where ground gas
103 was sampled on seven campaigns over a ten-year period to form a picture of daily and
104 seasonal fluctuations and, in doing so, developing many of the current techniques used to
105 monitor ground gas (Beaubien et al., 2013). Similar techniques have commenced at the
106 Glasgow Observatory and will be verified by comparing the results with those from previous
107 background gas studies (Beaubien et al., 2013; Carman et al., 2014; Ward et al., 2019; Li et
108 al, 2020 and results compiled by Jones et al., 2014). Signal to noise ratio (SNR) techniques
109 can then be used to determine which measurements are most likely to provide strong
110 indications of anomalies once investigation into the viability of using shallow geothermal
111 heat commences (Nickerson and Risk, 2013; Risk et al., 2015 and Tarakki et al., 2018).

112

113 Dixon and Romanak (2015) advance an alternative method, initially proposed by Romanak
114 et al. (2012), of identifying the source of ground gas and flux. They state that a site can be
115 characterised with one set of measurements using a process-based approach that indicates
116 the source of the gas based upon the stoichiometric relationship of the major gases so that
117 a tailored monitoring regime can then be established based upon this characterisation
118 taking into account the potential sources of ground gas. Further, they argue that baseline
119 studies are not appropriate in attributing gas leakage at every site and assert that the
120 process-based approach provides a suitable method for characterising anomalous gas. As
121 evidence of this Dixon and Romanak (2015) maintain that the baseline studies were not
122 useful in dealing with a gas leakage claim at Weyburn and that the process-based approach
123 was one of the only methods that successfully characterised the detected gas as originating
124 from a biological source.

125

126 Ground gas and gas flux measurements were collected during three discrete campaigns in
127 August 2018, May 2019 and October 2019 at four environmental baseline sites at the
128 Glasgow Observatory (**Figure 1**). The measurements were taken prior to research activities
129 and during preliminary site preparation (May 2019) and borehole drilling/construction
130 activities (October 2019). These measurements constitute the pre-operational background
131 gas values. This paper analyses the sampling techniques and results of the background gas
132 surveys, released as open data (National Geoscience Data Centre, 2021), in relation to the
133 site complexity and their applicability to low-enthalpy, shallow geothermal exploration and
134 compares them with the outcomes from the process-based analysis.

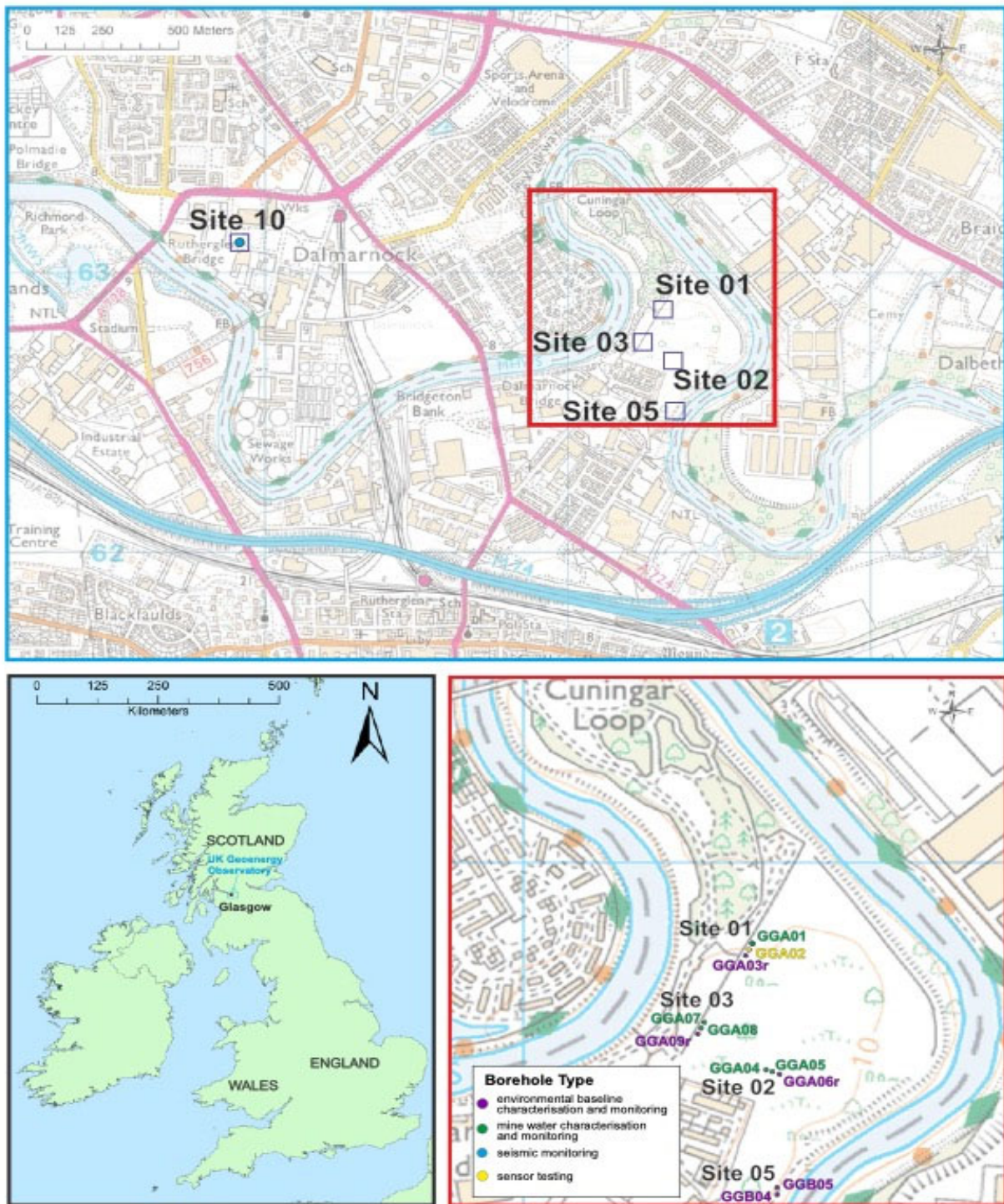


Figure 1 Location of the Glasgow Observatory including boreholes situated in the Cuningar Loop of the River Clyde (see red box). Contains Ordnance Survey data © Crown copyright and database rights. All rights reserved [2020] Ordnance Survey [100021290EUL]. Adapted from Monaghan et al. (2020).

137 2 Study Site

138

139 The Glasgow Observatory is one of three UK Geoenergy Observatories (UKGEOS) developed
140 to substantially improve our understanding of the subsurface environment and determine
141 the feasibility of carbon neutral technologies that harness geothermal energy resources as
142 well as investigating the potential for other low carbon energy technologies (UKGEOS,
143 2021). Investigations at the Glasgow Observatory will explore the processes and impacts of
144 using flooded, disused mines to extract geothermal heat (Monaghan et al, 2017).

145

146 The site is predominantly located in a meander of the River Clyde, named the Cuningar Loop
147 (**Figure 1**). It is now a public open space, but it has a complex history of industrial use. In this
148 area, the Upper Carboniferous sedimentary bedrock of the Scottish Coal Measures contains
149 a series of stacked coal seams that were mined between 1810 and 1934. The coal measures
150 are overlain by Quaternary glacial and post-glacial superficial deposits of variable thickness,
151 to about 35 m below surface level, and by a further 10-15 m of anthropogenic deposits,
152 made, filled and landscaped ground, relating to the various industrial uses of the site
153 (Monaghan et al., 2019a). The superficial deposits in the Cuningar Loop, from top down,
154 predominantly consist of alluvial sand and gravel from the River Clyde, part of the Gourrock
155 Sand Member, then a layer of the Paisley Clay Member, or Broomhouse Sand and Gravel
156 Formation, depending on the location within the Loop, which sits upon glacial till of the
157 Wilderness Till Formation, see **Figure 2** (Monaghan et al., 2019a). Detailed post-drill data
158 can be viewed in various publications on the UKGEOS website (2021).

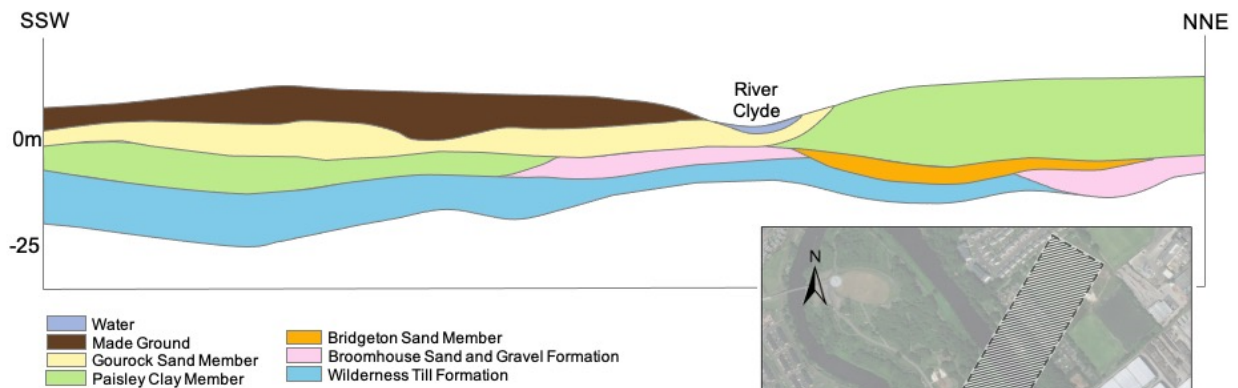


Figure 2 Example SSW–NNE cross-section (pre-drill) of superficial deposits in the vicinity of the research site adapted from Monaghan et al. (2019a). Vertical exaggeration x 3. Ground surface derived from NEXTMap Britain elevation data from Intermap Technologies. Hatched section with dashed outline on inset map shows area that information was obtained from to create cross-section. Sources for inset map: Esri, DigitalGlobe, GeoEye, i-cubed, USDA FSA, USGS, AEX, Getmapping, Aerogrid, IGN, IGP, swisstopo, and the GIS User Community.

160 There are eleven boreholes across the four Cuningar Loop sites; six that targeted the mine
 161 workings, a selection of which are planned to be part of a shallow mine water thermal heat
 162 loop, and five environmental baseline monitoring boreholes (**Figure 1** and **Figure 3**). There is
 163 also an additional seismic monitoring borehole about 1.5 kilometres to the west on the
 164 north bank of the River Clyde (Site 10 in **Figure 1**). The heat loop will be used to explore the
 165 ability to harness heat from within the shallow subsurface.

166

167 The surface character varies significantly across the four sites at Cuningar Loop. Some areas,
 168 at least superficially, appear relatively natural with more mature woodland, whereas in
 169 other areas the previous industrial and waste disposal land use is more apparent in an early
 170 succession landscape. Pictures of the sites showing the level of succession in the surface
 171 vegetation at the time of the soil chemistry survey can be seen in Fordyce et al. (2020). An
 172 industrial history of a waterworks, sand and gravel extraction, colliery workings and a
 173 mineral railway, all of which was infilled with demolition debris mean that rubble, coal spoil
 174 mounds and other buried waste material close to the surface is widespread across the
 175 entire site (Ramboll, 2018). In less complex settings, it is most likely that any migrating gas
 176 will use either natural or artificial preferential pathways, such as faults, boreholes or disused

177 wells (IPCC, 2005). The complexity of the shallow subsurface will affect these pathways, for
 178 instance, there may be reservoirs of escaped mine gas trapped below soils, natural and
 179 artificial, with low permeability (Jones et al., 2015), or there may be additional gas migration
 180 pathways through the shallow deposits to the surface. The process of drilling may have also
 181 created the potential for new gas migration pathways to surface.
 182

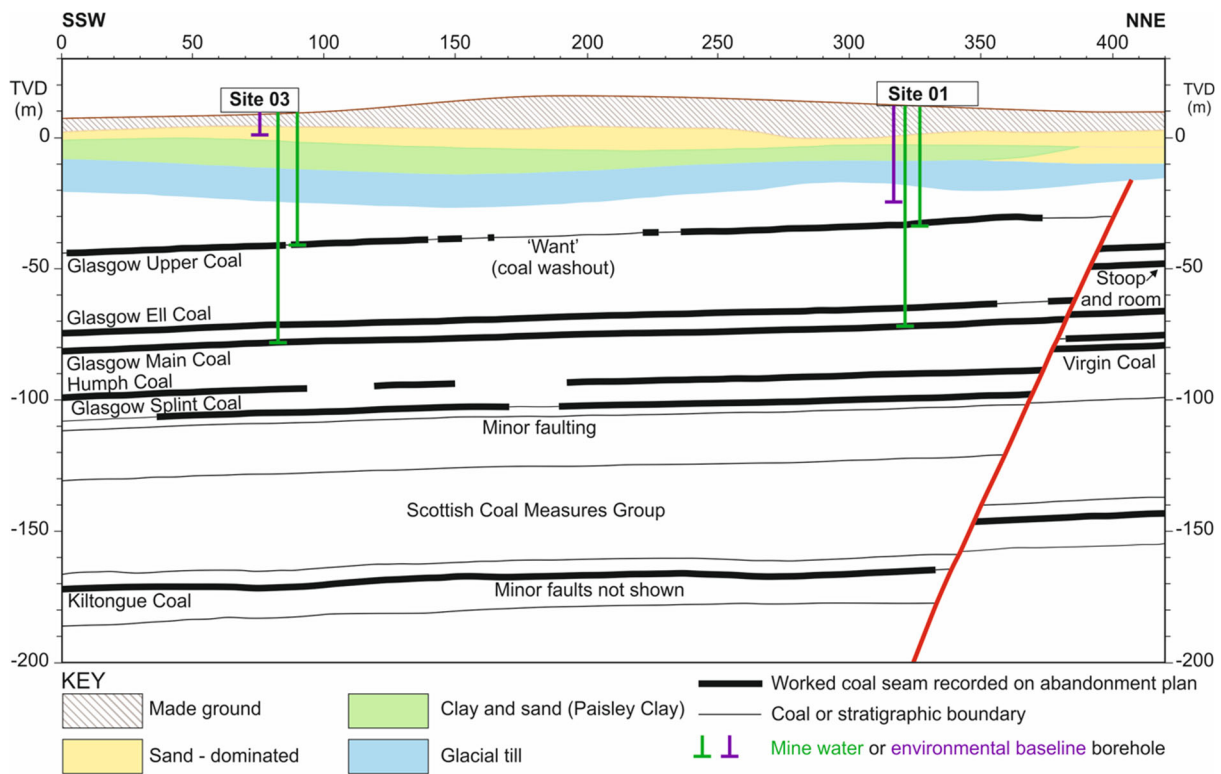


Figure 3 A pre-drill cross-section of part of the Glasgow Observatory illustrating how the mine water characterisation boreholes (green) intersect the mine workings and the relative position of the environmental boreholes (purple). The red line indicates an inferred fault (also see **Figure 4**) The depths are shown as True Vertical Depths (TVD) relative to Ordnance Datum. The horizontal axis is in metres (m) (Monaghan, 2019b).

183

184 3 Methods
 185 3.1 Survey design
 186

187 Point samples of ground gas and gas flux were taken at 83 locations in 20 m-spaced grids
 188 across the four sites (Site 1, Site 2, Site 3 and Site 5), taking into account faulted bedrock,
 189 superficial and made ground geology, particularly encompassing key locations such as,
 190 faults, legacy and new boreholes. 20 m-spaced grids were decided upon to balance the
 191 demands between covering a meaningful surface area at each of the sites and being of high
 192 enough resolution to offset the unpredictable impact that the made ground can have on the
 193 gas pathways. The idealised locations for the point measurements at each of the Glasgow
 194 Observatory sites are shown in **Figure 4**.

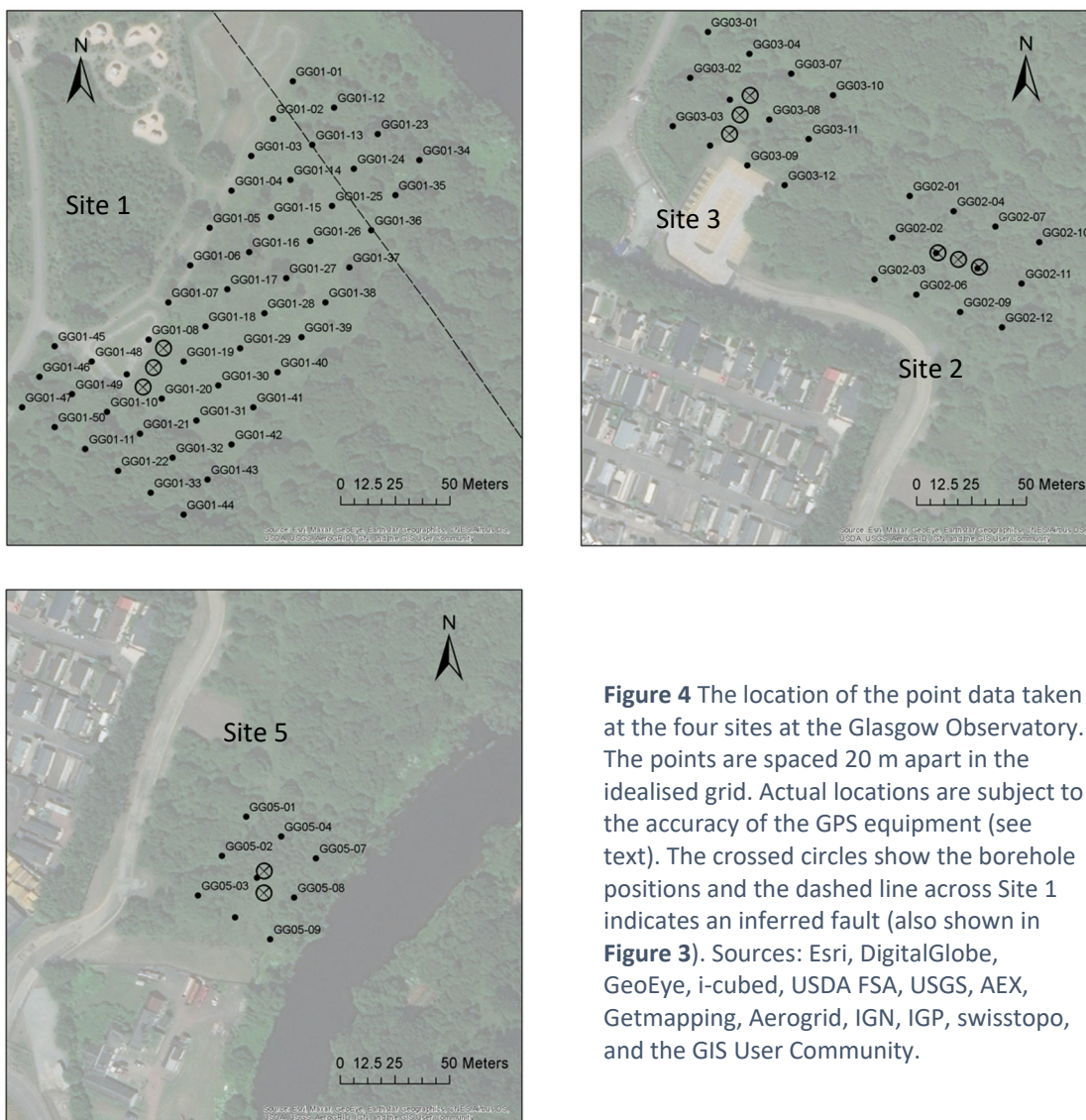


Figure 4 The location of the point data taken at the four sites at the Glasgow Observatory. The points are spaced 20 m apart in the idealised grid. Actual locations are subject to the accuracy of the GPS equipment (see text). The crossed circles show the borehole positions and the dashed line across Site 1 indicates an inferred fault (also shown in **Figure 3**). Sources: Esri, DigitalGlobe, GeoEye, i-cubed, USDA FSA, USGS, AEX, Getmapping, Aerogrid, IGN, IGP, swisstopo, and the GIS User Community.

195

196 3.2 Ground gas concentrations

197

198 Ground gas was sampled using thick-walled, stainless steel probes, with external diameter
199 of 8 mm, that were driven into the ground to a maximum depth of 80 cm below ground
200 level to avoid the dilution of ground gas by atmospheric air.

201

202 Samples of ground gas were pumped directly to a Geotechnical Instruments GA 5000
203 portable gas analyser which was attached to the probes to determine the major
204 components of ground gas. The instrument produces CO₂, CH₄ and O₂ concentration data
205 (volume percentage, %) and a H₂S concentration (parts per million, ppm). It is also adapted
206 to measure H₂ concentration (ppm) and calculates a 'residual balance' as a percentage
207 concentration, such that:

208

209 Residual balance = 100% - (%CH₄ + %CO₂ + %O₂)

210

211 The residual balance is roughly equivalent to nitrogen (N₂) concentrations in most
212 circumstances and is used in this study as a proxy for N₂.

213

214 In addition, a Huberg Laser One analyser was used to measure the CH₄ concentration
215 directly from the probe in ppm.

216

217 Instrument specifications can be found at the relevant manufacturer websites (Geotech,
218 n.d.; QED, 2020) and Appendix A. The ground gas instruments are serviced and calibrated
219 regularly by the manufacturer and additional quality control checks are made before
220 deployment using in-house methods, as well as in the field, as required, to maintain data
221 quality. The data reported is taken directly from these instruments without further
222 manipulation.

223

224 3.3 CO₂ and CH₄ flux

225

226 Gas flux was measured at the ground surface using a closed-loop accumulation chamber
227 (net volume 2.756 x 10⁻³ m³) attached to a West Systems flux meter, equipped with a Li-

228 COR[®] model LI820 analyser (Li-COR, n.d. and Appendix A). The gas flux data reported is
229 converted from mol m⁻² d⁻¹ to g m⁻² d⁻¹.

230

231 3.4 Stable isotopes of carbon in CO₂ ($\delta^{13}\text{C}_{\text{V-PDB}}$)

232

233 Where measured ground gas parameters were notably different to neighbouring samples,
234 additional ground gas samples were collected for $\delta^{13}\text{C}$ isotope analysis. The analysis was by
235 Iso-Analytical Limited, UK using their documented GC-IRMS method to calculate a per mille
236 $\delta^{13}\text{C}$ ratio normalised to the V-PDB (Vienna Pee Dee Belemnite) standard.

237

238 In all, isotope samples were taken at two of the probe locations as part of the August 2018
239 campaign and four locations during the May 2019 campaign. Research by Flude et al. (2017)
240 attributing isotope results to biogenic and geogenic sources was used to help with the
241 interpretation of these measurements.

242

243 3.5 Data interpretation

244

245 Given the subsurface complexity at the Glasgow Observatory due to the various previous
246 uses of the location, referred to in section 2, it is possible that each environmental baseline
247 site 1-5 has a significantly different gas profile. To establish whether the site results should
248 be treated separately a one-way analysis of variance (ANOVA) evaluation was used to
249 identify whether there was a statistical difference between the measurements at each site.
250 This test was applied to the groups of CO₂ concentration and CO₂ flux measurements from
251 each site and compared between the four sites. A statistical difference is identified by
252 comparing the *F*-value, a value measuring the separation between the distributions of each
253 sample group, with an *F*-critical value that identifies that there is a difference between the
254 groups at the 95% confidence level. This same test was used to determine if there was a
255 significant difference between the campaigns for the same two gas measurements. If a
256 statistical difference was identified then pairwise comparisons were made between the
257 sites and campaigns using the post-hoc, Tukey-Kramer analysis, also at the 95% confidence
258 level, to establish where the differences lay. These analyses were chosen because they
259 establish whether there is a difference between the means of unrelated, categorical groups

260 of measurements; this analysis was applicable for both the geographical (sites) and
261 temporal (campaigns) groups.

262

263 In addition to comparing the range, mean, median and standard deviation of the ground gas
264 concentrations and fluxes, a process-based approach (Romanak et al., 2012) was also
265 applied to ground gas concentrations to assist in determining the origin of CO₂. The process-
266 based analysis is a stoichiometric approach that evaluates ground gas concentrations of CO₂
267 against O₂, the N₂/O₂ ratio against CO₂ and CO₂ against N₂ to determine the biological or
268 geological origin of CO₂ (**Figure 5**). Datapoints falling in the orange (lowest) area suggest
269 that the reduced level of detectable CO₂ is due to CO₂ dissolution, whereas datapoints
270 falling within the areas above the top, biological respiration line suggest an additional CO₂
271 input. Datapoints falling between the two lines are considered normal background levels of
272 CO₂ as a result of biological and geological processes.

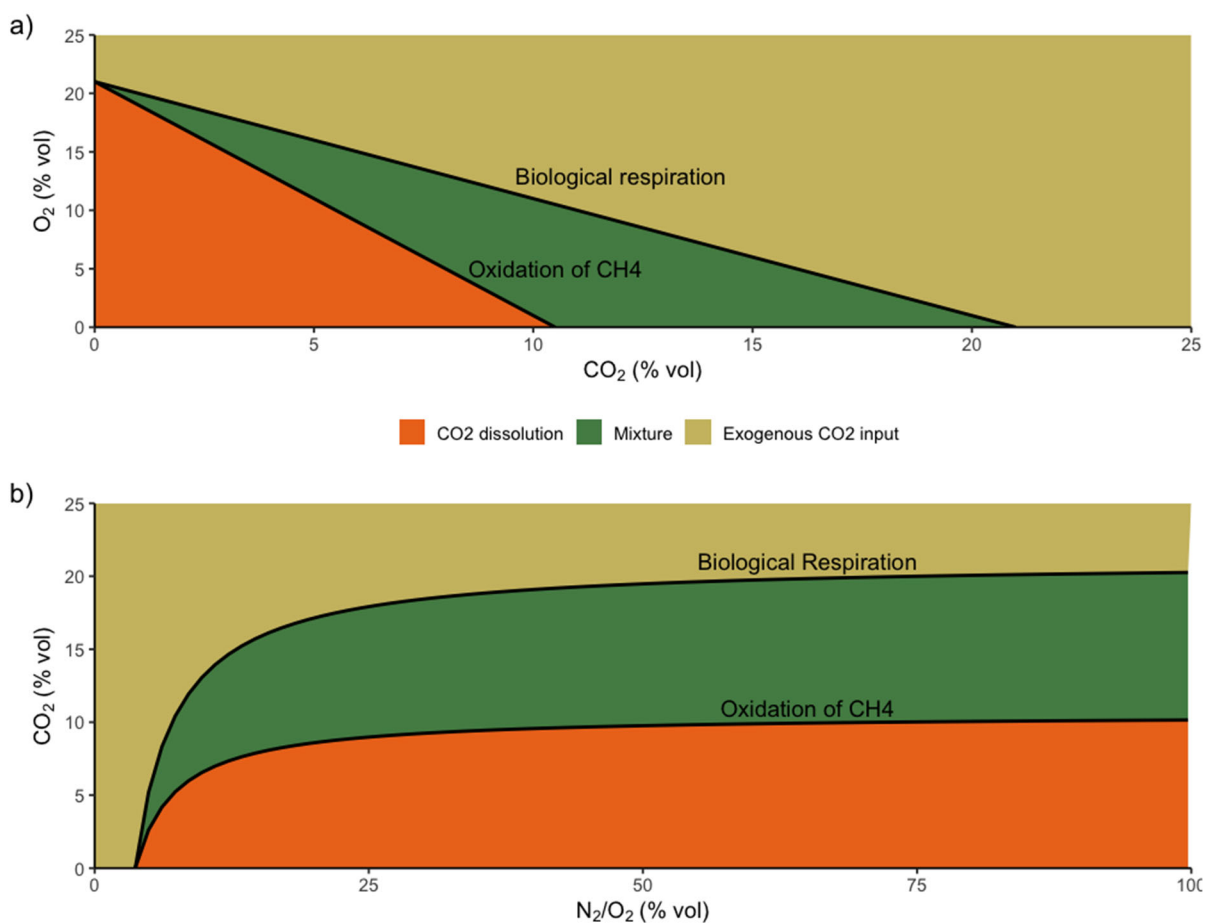


Figure 5 Interpretation of a) the O₂ and CO₂ data and b) CO₂ and N₂/O₂ developed by Romanak et al. (2012). The plotted lines are created by the stoichiometric relationship for biological respiration and oxidation of CH₄, respectively.

273

274 4 Results and Analysis

275 4.1 Results

276

277 Details of the measurements obtained in each survey and a summary of data are given in
278 **Tables 1 to 3**; the complete datasets are available at the National Geoscience Data Centre
279 (2021). Across the four Glasgow Observatory sites, the idealised grids totalled 83 sample
280 points. In practice, it was sometimes not possible to obtain data for all parameters at all
281 sample points due to prevailing ground conditions e.g., buried material, made ground,
282 ongoing works or saturated ground. A handheld Garmin GPS was used to locate the British
283 National Grid coordinates and locations are accurate to 5 m in ideal conditions. Where it
284 was not possible to obtain a GPS signal because of obstruction by vegetation/tree canopy
285 etc, grid coordinates were located using measuring tape. CH₄ flux is not reported as we
286 were unable to detect any quantifiable CH₄ flux across the three surveys, apart from one
287 measurement of 0.282 g m⁻² day⁻¹ recorded at GG01-40 in October 2019 (**Figure 6**); all other
288 measurements were below the instrument's lower detection limit of 0.08 g CH₄ m⁻² day⁻¹.

289

290 **Table 1** Summary of August 2018 survey data. n=number of sample points. Reference to "<0.5" or "<1"
291 denotes that the measurements were below the instruments' detection limits.

Gas Measured	n	Mean	Median	Standard Deviation	Maximum	Minimum
CH ₄ (ppm)	67	1.9	1.9	0.5	3.8	<0.5
CO ₂ (% vol)	68	3.3	2.6	2.7	12.4	<0.5
O ₂ (% vol)	68	17.6	18.7	4.2	22.7	0.9
H ₂ (ppm)	68	2.0	1.0	3.9	23.0	<1
H ₂ S (ppm)	68	<1	<1	0.1	1.0	<1
Balance (N ₂) (% vol)	68	79.1	78.6	1.8	88.9	76.3
N ₂ /O ₂	68	6.2	4.2	11.6	98.8	3.4
CO ₂ flux (g m ⁻² day ⁻¹)	74	30.5	28.1	14.9	81.7	10.9

292

293

294 **Table 2** Summary of May 2019 survey data. n=number of sample points. Reference to “<0.5” or “<1” denotes
 295 that the measurements were below the instruments’ detection limits.

Gas Measured	n	Mean	Median	Standard Deviation	Maximum	Minimum
CH ₄ (ppm)	58	1.4	1.6	1.1	8.2	<0.5
CO ₂ (% vol)	58	4.0	3.2	3.2	17.9	<0.5
O ₂ (% vol)	58	16.5	17.4	3.6	20.5	1.6
H ₂ (ppm)	58	12.9	6.0	17.2	65.0	<1
H ₂ S (ppm)	58	0.4	<1	0.5	1.0	<1
Balance (N ₂) (% vol)	58	79.5	79.3	1.0	83.5	76.8
N ₂ /O ₂	58	5.8	4.6	6.1	50.3	3.8
CO ₂ flux (g m ⁻² day ⁻¹)	59	22.7	21.9	16.1	79.0	-7.2*

296 *negative flux implies net transfer of CO₂ from atmosphere to soil.
 297

298 **Table 3** Summary of October 2019 survey data. n=number of sample points. Reference to “<0.5” or “<1”
 299 denotes that the measurements were below the instruments’ detection limits.

Gas Measured	n	Mean	Median	Standard Deviation	Maximum	Minimum
CH ₄ (ppm)	62	4.7	2.4	20.5	163.0	<0.5
CO ₂ (% vol)	62	5.1	4.9	3.6	18.0	<0.5
O ₂ (% vol)	62	16.0	16.2	4.1	21.8	2.8
H ₂ (ppm)	62	3.7	<1	10.1	60.0	<1
H ₂ S (ppm)	62	0.9	<1	5.0	38.0	<1
Balance (N ₂) (% vol)	62	78.9	78.4	1.5	86.4	76.6
N ₂ /O ₂	62	5.7	4.9	3.9	28.3	3.6
CO ₂ flux (g m ⁻² day ⁻¹)	65	12.6	11.6	5.8	35.6	3.5

300
 301 Ranges of ground gas concentrations of CO₂, H₂ and O₂, along with CO₂ flux, are shown in
 302 **Figure 7a** to d. **Figures Figure 8** and **Figure 9** show the spatial distribution of CO₂
 303 concentrations and CO₂ flux at each of the four sites in August 2018, May and October 2019.
 304 **Figure 10** shows the spatial distribution of H₂ for the three campaigns.

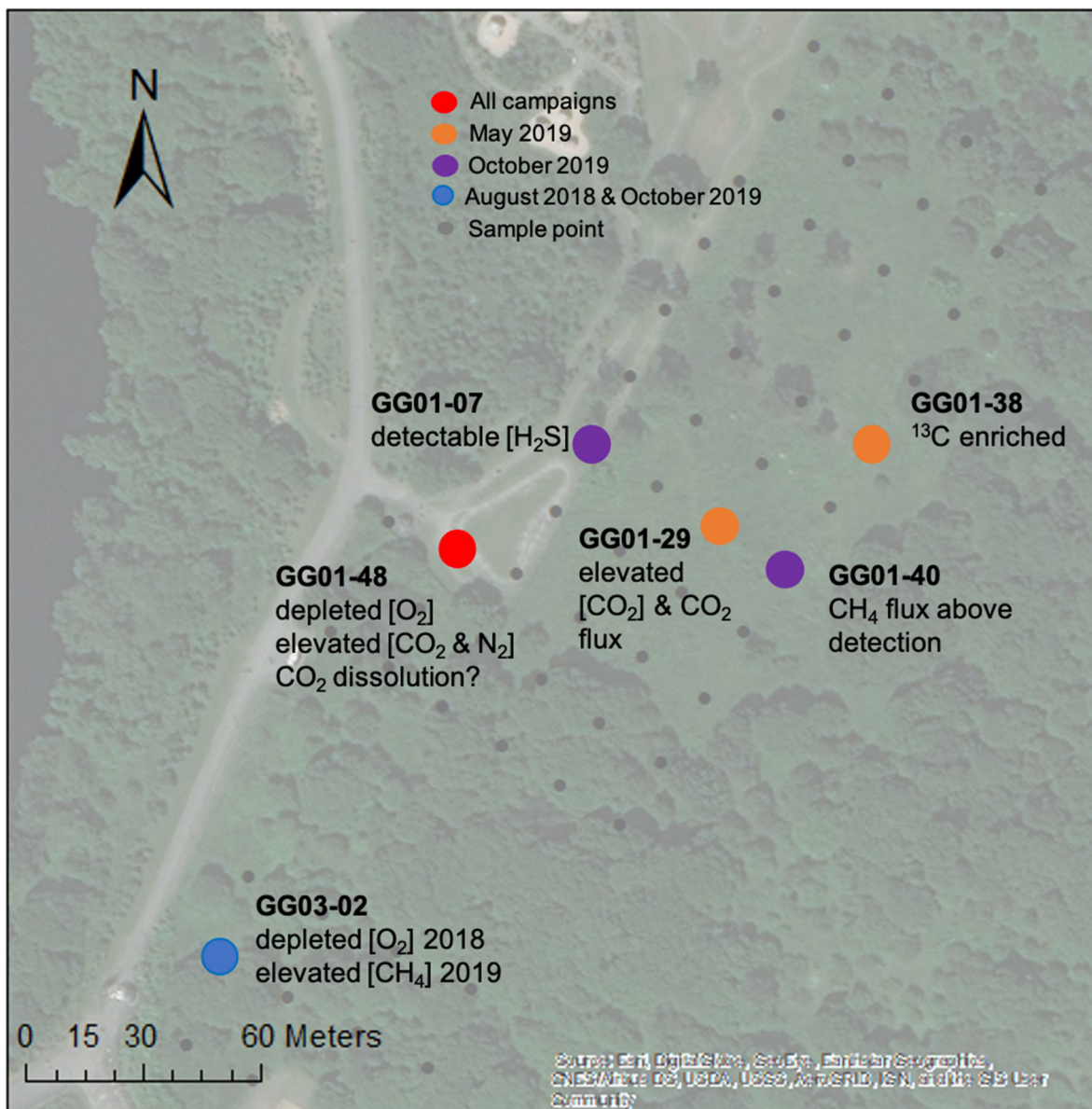


Figure 6 Individual sample points highlighted in the text. Square brackets indicate the values for gas concentrations. This summary figure is provided for convenience, it is not intended to convey any significance other than where explicitly stated in the text. Sources: Esri, DigitalGlobe, GeoEye, i-cubed, USDA FSA, USGS, AEX, Getmapping, Aerogrid, IGN, IGP, swisstopo, and the GIS User Community.

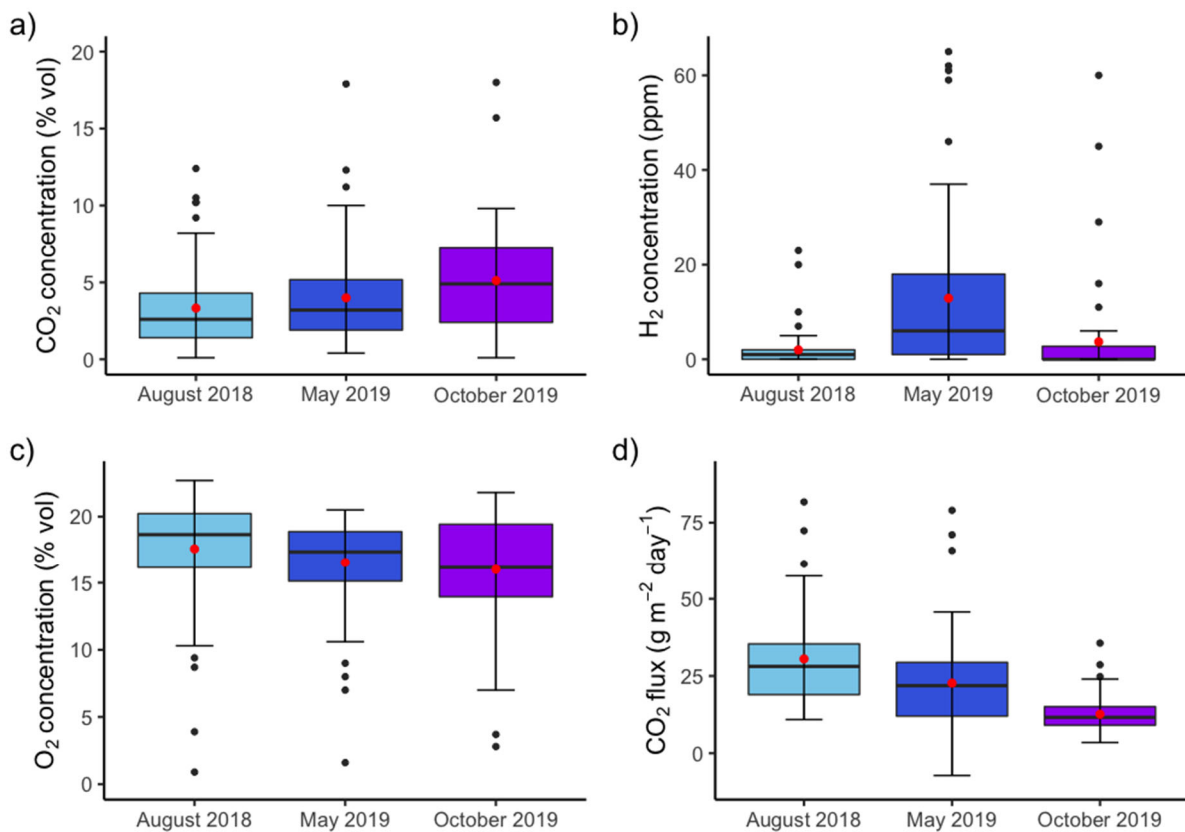
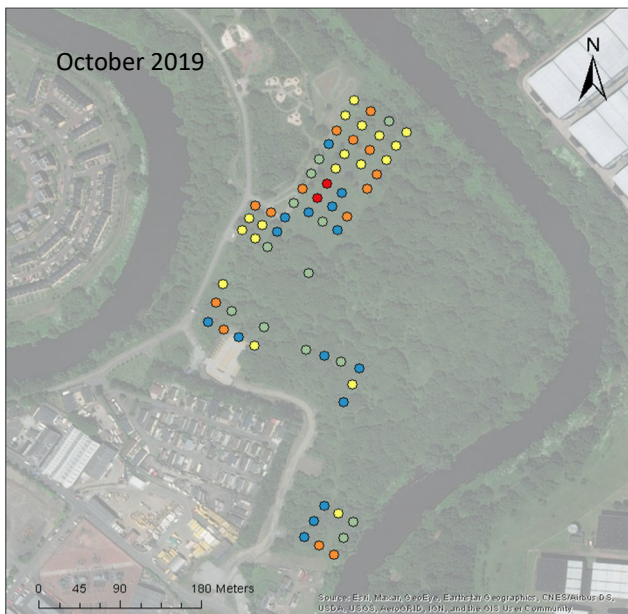
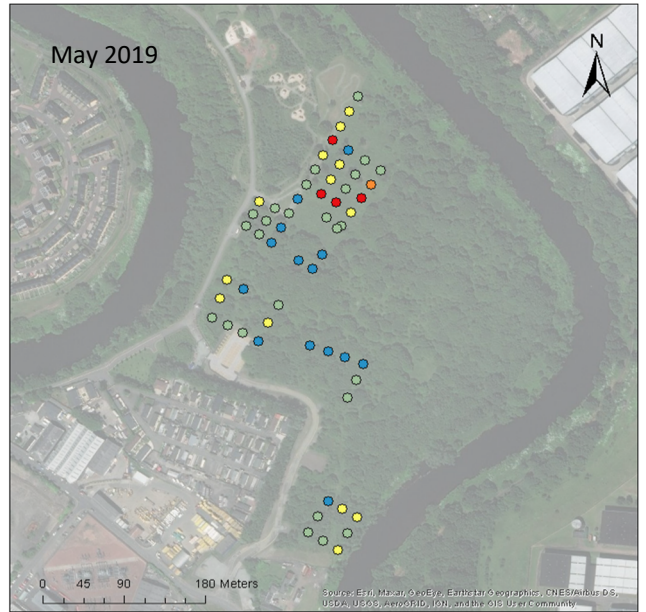
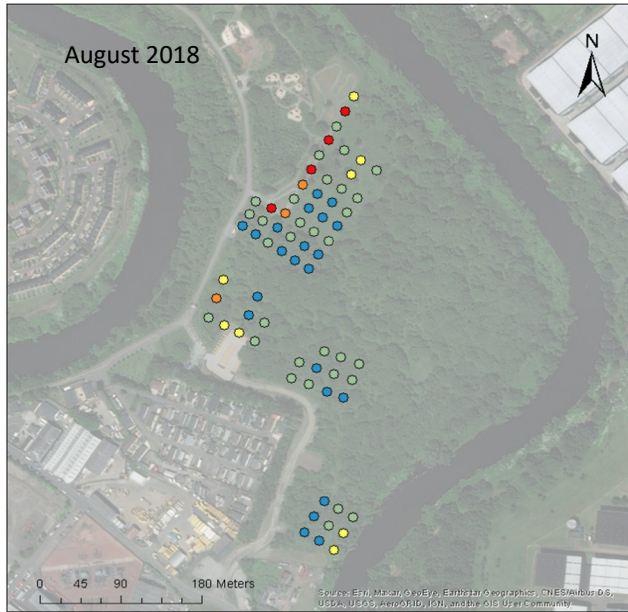


Figure 7 Boxplots comparing the range of baseline observations for August 2018, May and October 2019 for a) CO₂ concentration, b) H₂ concentration, c) O₂ concentration and d) CO₂ flux. The red point shows the mean of each set of observations, the black horizontal line shows the median value, the black points show outlier observations and the whiskers represent 1.5 times the standard deviation. The CO₂, H₂ and O₂ concentrations were analysed by the GA5000 gas analyser, the CO₂ flux was measured by West Systems flux meter.

307 $\delta^{13}\text{C}$ stable isotope values for CO₂ in ground gas samples taken in August 2018 at GG01-07
 308 and GG01-48 were -23.82 and -26.31‰ $\delta^{13}\text{C}_{\text{V-PDB}}$, respectively. Four further measurements
 309 taken in May 2019 at GG01-10, GG01-38, GG02-11 and GG03-06 were -23.59, -16.76, -25.00
 310 and -26.10‰ $\delta^{13}\text{C}_{\text{V-PDB}}$, respectively (**Figure 11**).



GA5000 CO₂ concentration
(% vol)

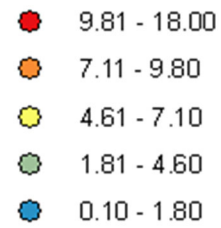


Figure 8 The CO₂ concentration measurements taken at Sites 1, 2, 3 and 5 by GA 5000 for August 2018, May and October 2019. Sources: Esri, DigitalGlobe, GeoEye, i-cubed, USDA FSA, USGS, AEX, Getmapping, Aerogrid, IGN, IGP, swisstopo, and the GIS User Community.

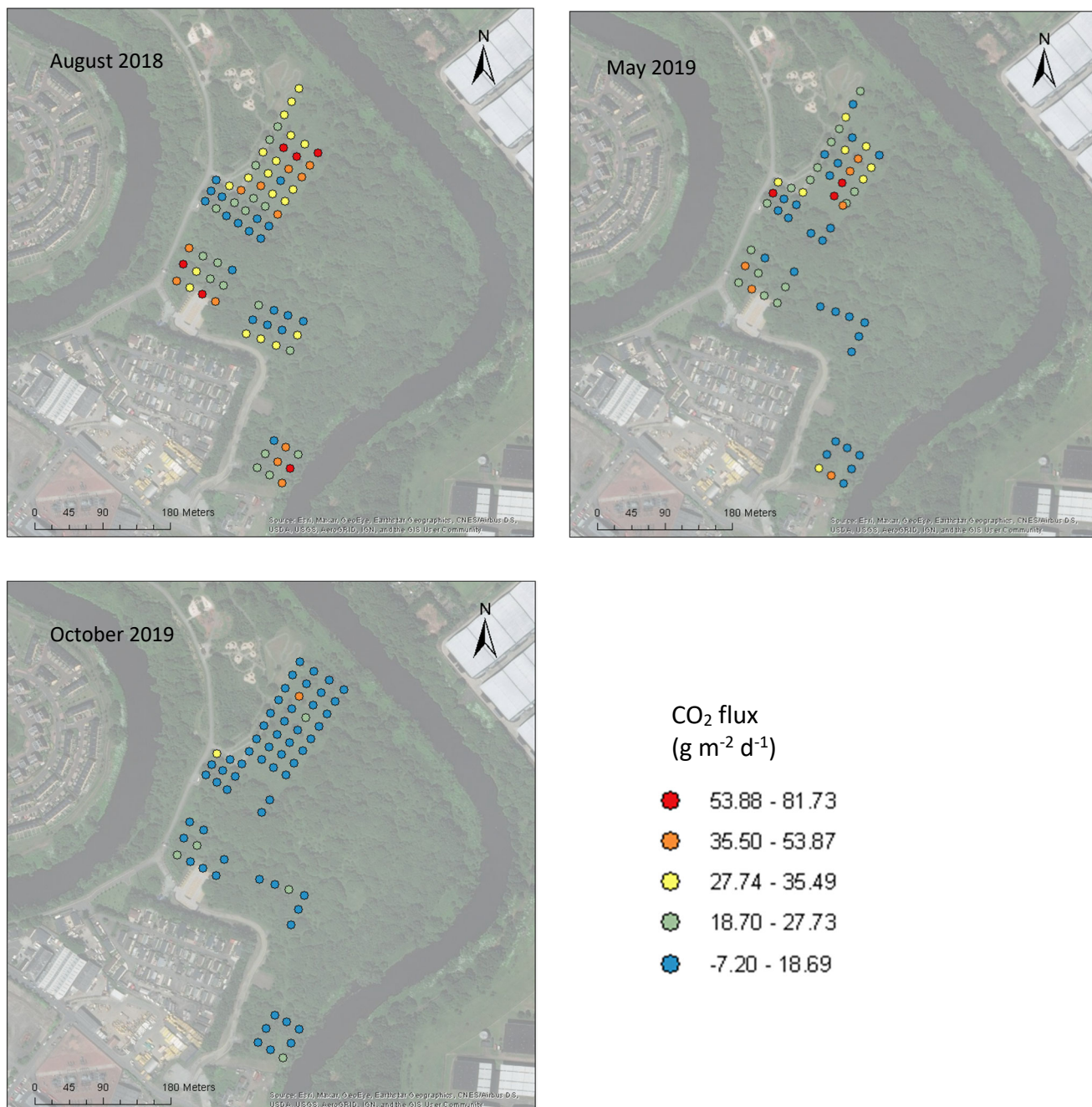


Figure 9 The CO₂ flux measured at Sites 1, 2, 3 and 5 by the West Systems flux meter for August 2018, May and October 2019. Sources: Esri, DigitalGlobe, GeoEye, Earthstar Geographics, CNES/Airbus DS, USDA, USGS, AeroGRID, IGN, and the GIS User Community.

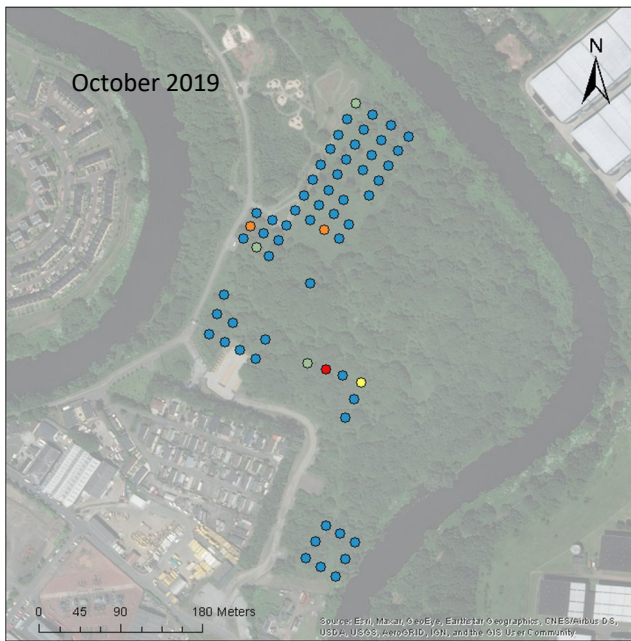
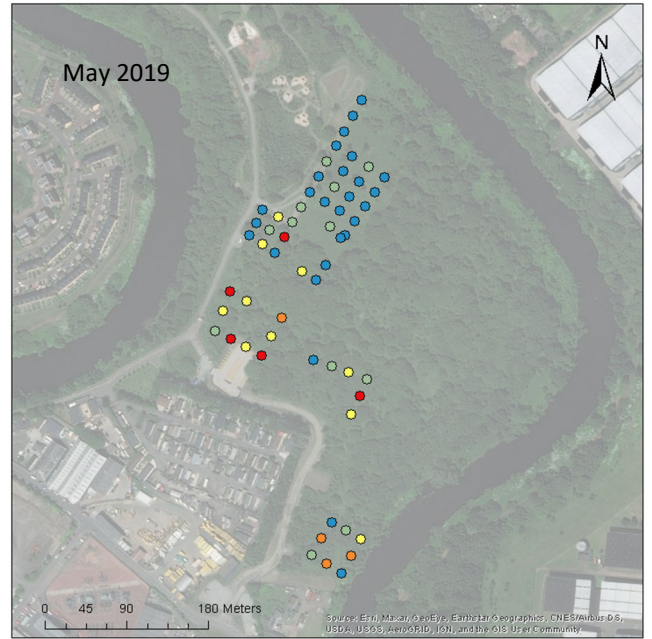
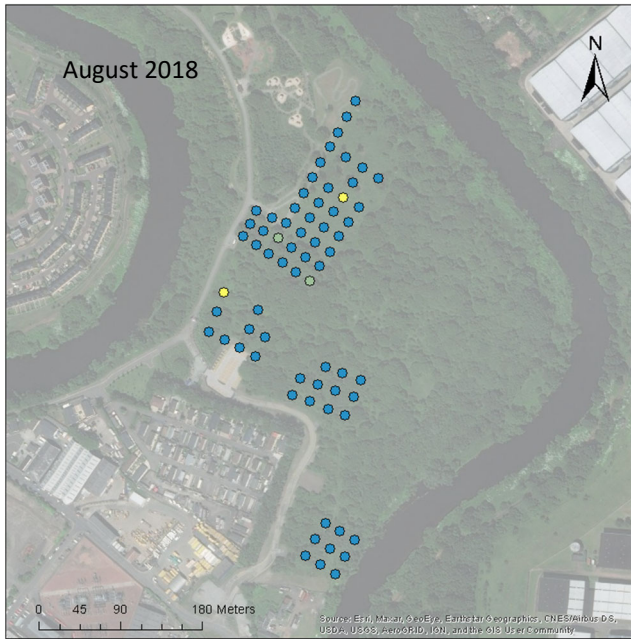


Figure 10 The H₂ measurements taken at Sites 1, 2, 3 and 5 by GA 5000 for August 2018, May and October 2019. Sources: Esri, DigitalGlobe, GeoEye, Earthstar Geographics, CNES/Airbus D.S., USDA, USGS, AeroGRID, IGN, and the GIS User Community.

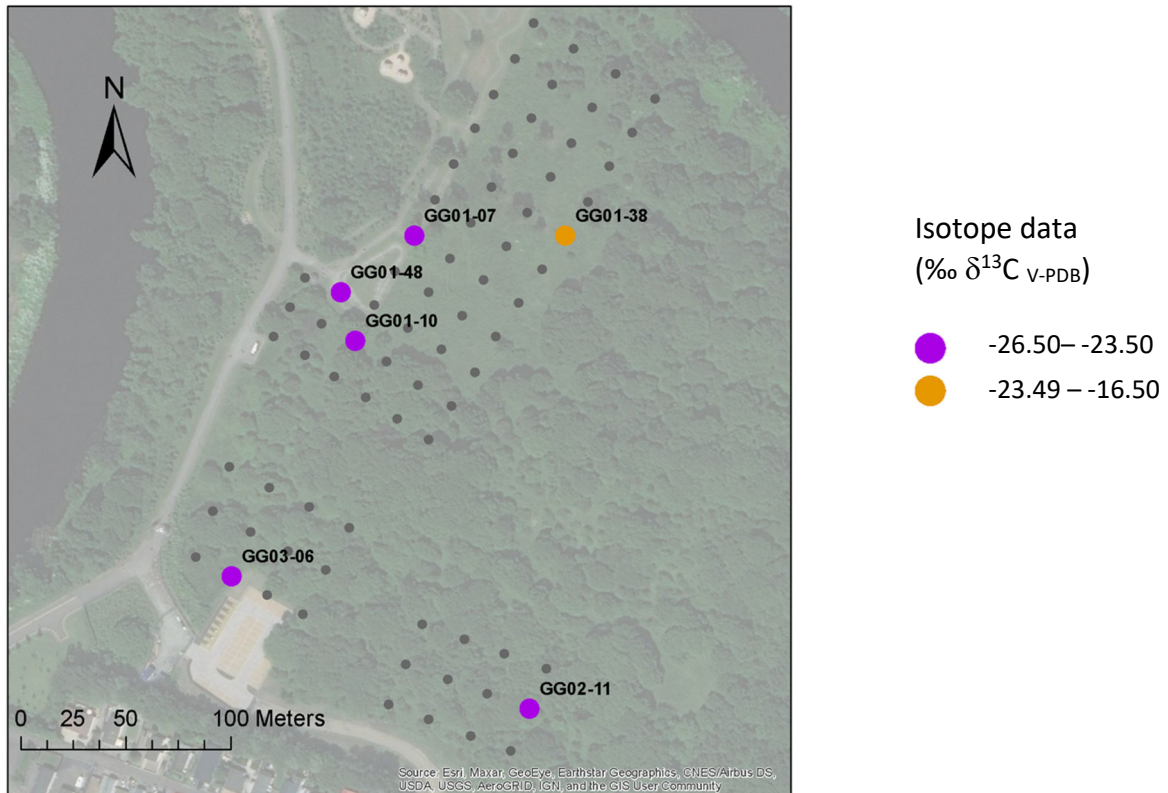


Figure 11 Spatial distribution of the six stable isotope samples. Samples from locations GG01-07 and GG01-48 were taken during the August 2018 campaign and samples GG01-10, GG01-38, GG02-11 and GG03-06 were taken during the May 2019 campaign. The grey circles indicate the position of the sample points. Sources: Esri, DigitalGlobe, GeoEye, i-cubed, USDA FSA, USGS, AEX, Getmapping, Aerogrid, IGN, IGP, swisstopo, and the GIS

314

315 4.2 Analysis

316 4.2.1 CO₂ comparison between sites

317

318 Using the ANOVA analysis for each of the campaigns, August 2018, May 2019 and October
 319 2019, *F*-values comparing the ground gas CO₂ concentration data between the four sites
 320 were 0.61, 1.74 and 1.79 with corresponding *F*-critical values of 2.75, 2.78 and 2.76 at a 95%
 321 level of confidence, respectively. *F* values comparing the CO₂ flux data between the four
 322 sites for the three campaigns were 2.67, 2.09 and 0.12 compared with *F*-critical values of
 323 2.74, 2.77 and 2.75 for a 95% level of confidence. This analysis indicates the absence of a
 324 statistical difference for the between-site data. Therefore, the measurements for CO₂
 325 concentration and CO₂ flux can be treated as single populations for each of the campaigns
 326 from this point, although notable measurements will be highlighted.

327

328 4.2.2 CO₂ comparison between campaigns

329

330 The ranges of the CO₂ ground gas concentrations across the three campaigns are similar, i.e.
331 0.1– 12.4% vol for August 2019, 0.4– 17.9% vol for May 2019 and 0.1– 18.0% vol for October
332 2019, although the latter campaign has a slightly wider spread across the central 50% of the
333 data (**Figure 7a**). The mean and median CO₂ concentrations increase stepwise from August
334 2018 to October 2019, from 3.3 to 5.1 % vol and medians from 2.6 to 4.9 % vol (**Tables 1, 2**
335 and **3** and **Figure 12**). One-way ANOVA analysis suggests that there is a statistical difference
336 between the CO₂ concentrations for the campaigns (*F*-value of 5.19 compared with an *F*-
337 critical value of 3.04 for a 95% confidence level) but the post-hoc Tukey-Kramer test, shows
338 that only the August 2018 and October 2019 data are statistically different.

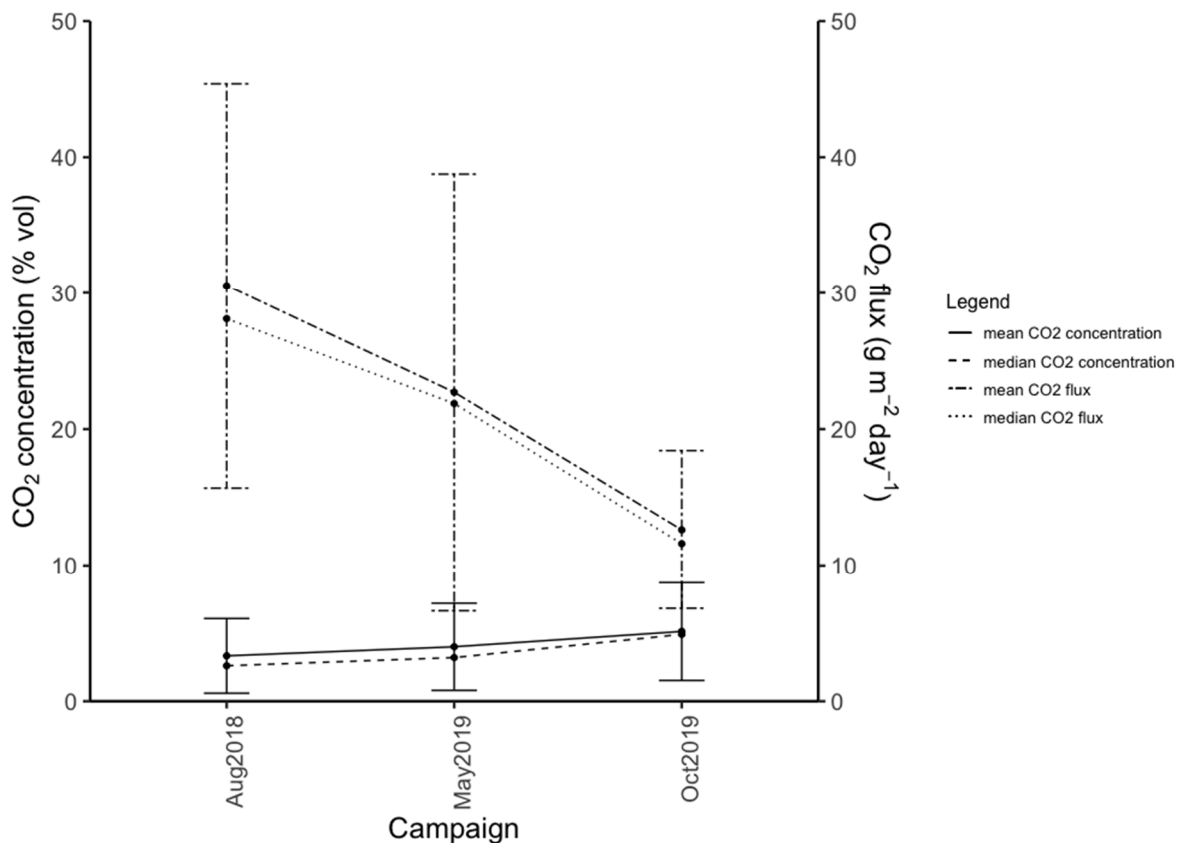


Figure 12 The mean and median CO₂ concentration and flux for the three campaigns. The CO₂ flux data was analysed using the West Systems flux meter equipped with a Li-COR® model LI820 analyser. The CO₂ concentration data was analysed using Geotechnical Instruments GA 5000. The error bars show 1 s.d.

339

340 Inversely to the ground gas CO₂ concentrations, the overall mean and median values for CO₂
341 flux reduce progressively from August 2018 to October 2019 (means 30.5 – 12.6 g m⁻² day⁻¹;
342 medians 28.1 – 11.6 g m⁻² day⁻¹ (**Figure 7a** and **d** and **Tables 1, 2** and **3** and **Figure 12**).

343

344 There is some similarity between the upper end of the range of values and the middle 50%
345 of the spread for the CO₂ flux measurements between the first two campaigns with ranges
346 of 10.9 – 81.7 g m⁻² day⁻¹ for August 2018 and -7.2 – 79.0 g m⁻² day⁻¹ for May 2019, but the
347 October 2019 campaign has a tighter spread of measurements, between 3.5 – 35.6 g m⁻²
348 day⁻¹ (**Figure 7d**). Analysis using ANOVA shows that there is a statistically significant
349 difference in the data across the three campaigns for a 95% confidence level with an *F*-value
350 of 33.03 compared with an *F*-critical value of 3.04. Post-hoc Tukey-Kramer analysis shows a
351 statistical significance between each pairing of campaigns.

352

353 Although the ground gas and gas flux data does not neatly fit the assumption for ANOVA,
354 that the data is normally distributed, the test does have some tolerance to non-normality
355 (Glass et al., 1972). In addition, all the data that shows a statistical difference does so at the
356 higher 99% confidence level, so it was not considered necessary to interrogate the results
357 from this statistical approach further.

358

359 4.2.3 Ground gas

360

361 Apart from a small number of measurements, most notably one at GG03-02 of 163 ppm in
362 October 2019 (**Figure 6**), CH₄ concentrations in ground gas were found to be low in all three
363 campaigns with means of 1.9, 1.4 and 4.7 ppm for the August 2018, May 2019 and October
364 2019 campaigns, respectively. If the one outlying measurement was excluded from the
365 latter campaign, the mean for the October 2019 would be 2.1 ppm with a standard
366 deviation of 1.2 ppm. This is more consistent with other findings, nonetheless the
367 measurement has been retained in the dataset. These results are within the range expected
368 for atmospheric dry air, and do not suggest significant mine gas inputs to the ground gas. It
369 is likely that any CH₄ that had been present has since been oxidised or, if still present in the
370 subsurface, it was trapped beneath an impermeable layer, such as rock, clay, water or waste
371 material, that prevents its migration to the near surface measurement points (Dixon and

372 Romanak, 2015). Similarly, there was almost no H₂S detected at the Glasgow Observatory
373 over the three campaigns, apart from one value of 38 ppm in October 2019 at GG01-07
374 (Figure 6).

375

376 There was some detection of H₂ in ground gas, particularly in May 2019 (Figure 10), where
377 the measurements were distributed across the four sites, although Site 2 showed the
378 highest concentration of measurements above 26 ppm. There were only three other
379 measurements in this category, and they were all taken in October 2019 at Sites 1 and 3.
380 Molecular hydrogen is highly prevalent in nature, usually from deep geological processes
381 (Zgonnik, 2020), however, it is unusual to detect molecular hydrogen in soils as it is usually
382 sorbed by the soil or consumed by microorganisms. Anthropogenic sources include the
383 interaction of water with finely ground metal, such as aluminium (Wilson et al., 2010),
384 which is possible given the history of the site. Hydrogen is also produced in the charging of
385 lead acid batteries, used for activities such as haulage in the mining industry, and from the
386 corrosion of other metals, such as magnesium or steel, particularly in acid. At present the
387 provenance of H₂ is uncertain, but although the highest levels of H₂ detected, at 65 and 60
388 ppm in May and October 2019, respectively, are more than 100 times that of the
389 atmospheric concentration for dry air, they are nearly three orders of magnitude below the
390 lower explosive or flammable limit in air, which is between 5% and 15% (Appleton, 2011;
391 Wilson et al., 2010).

392

393 Given that the concentrations of these three 'coal mine gases' (CH₄, H₂S and H₂) were low it
394 is unlikely that their presence in ground gas is due to migration from the former coal mines.

395

396 In relation to the stable carbon isotopes of CO₂, $\delta^{13}\text{C}_{\text{V-PDB}}$, five of the six sample values range
397 from -23.59 to -26.31‰ $\delta^{13}\text{C}_{\text{V-PDB}}$, consistent with the values for soil respired CO₂ (Flude et
398 al., 2017). The apparent outlier, -16.76‰ $\delta^{13}\text{C}_{\text{V-PDB}}$ for GG01-38 in May 2019 (Figure 6), is
399 still consistent with background soil CO₂ measurements for Carbon Capture and Storage
400 (CCS) pilot sites according to the index developed by Flude. Interpretation of carbon isotope
401 analysis can cause confusion when viewed in isolation due to the overlap between $\delta^{13}\text{C}_{\text{V-PDB}}$
402 signatures (Flude et al., 2017). This is highlighted by Dixon and Romanak (2015), particularly

403 in respect of the confusion at Weyburn. Therefore, the results from the Glasgow
404 Observatory samples were used in conjunction with other evidence, particularly as the
405 original isotopic signature (e.g. of mine gas) is not known.

406

407 All three campaigns exhibit a wide range of O₂ measurements, although they have similar
408 mean values, albeit declining chronologically (**Figure 7c**). The comparable spread of the data
409 across the campaigns is also confirmed by the size of the standard deviations, ranging from
410 3.6% vol to 4.2% vol. Most of the low ground gas O₂ concentrations (less than 10% vol)
411 occur at Site 1. This indicates that Site 1 is the most active area in terms of oxidation, which
412 is borne out by the CO₂ concentration data. The exception is one measurement of O₂ at
413 GG03-02 in August 2018 (**Figure 6**), which was 8.7% vol, where the highest CH₄
414 measurement was obtained.

415

416 **Tables 1, 2 and 3** and **Figure 13** also show that the balance of the unaccounted ground gas
417 (proxy N₂) concentration ranges and means are similar for the three surveys. The mean
418 values were slightly above atmospheric concentration of N₂ for dry air.

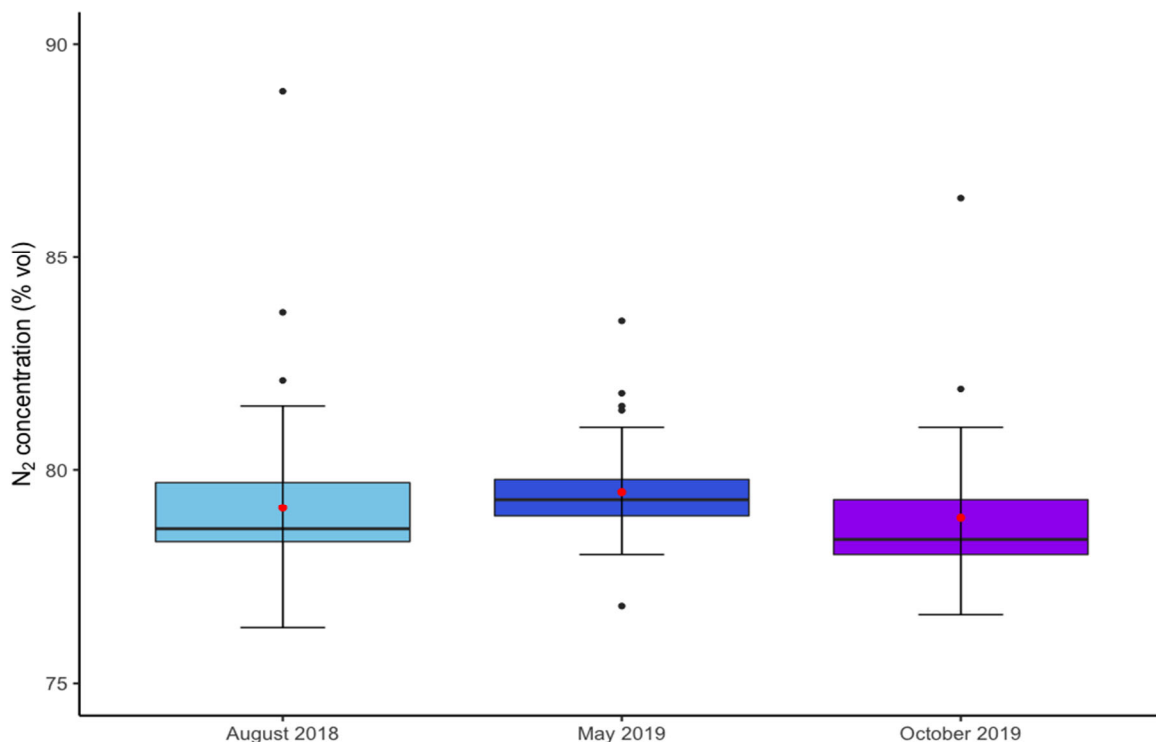


Figure 13 Boxplot comparing the range of baseline observations for August 2018, May and October 2019 for N₂. The red point shows the mean of each set of observations, the black horizontal line shows the median value, the black points show outlier observations and the whiskers represent 1.5 times the standard deviation. The N₂ concentrations were analysed by the GA5000 gas analyser.

419

420 One location of note is GG01-48, one of the more westerly locations in Site 1, next to the
421 bicycle track (**Figure 4** and **Figure 6**). This location consistently saw the highest ground gas
422 N₂ concentration for each of the campaigns: 88.9% vol for August 2018, 83.5% vol for May
423 2019 and 86.4% vol for October 2019. This is coupled with low O₂ concentrations, 12.9 and
424 7.0% vol for May and October 2019, respectively, and very low O₂, 0.9% vol, in the August
425 2018 campaign. The CO₂ concentrations at this point were 10.2%, 3.3% and 7.3% for the
426 August 2018, May and October 2019 campaigns, respectively. Stable isotope analysis of the
427 sample from this location suggests that the CO₂ is of biological origin (-26.31‰ δ¹³C_{V-PDB}).
428 The presence of CO₂, low O₂ and a high proportion of N₂ may indicate that oxidation of CH₄
429 is occurring at this point. Another hypothesis is that denitrification, under anoxic conditions,
430 is occurring as this is an acceptable alternative to sustain microbial metabolic processes,
431 where oxygen is in short supply, (Castaldi, 2000; Beaubien et al., 2015 and Chapin et al.,
432 2012). As a result, elevated levels of N₂ would be observed in these areas, particularly if the
433 gas was not able to escape. However, there is a greater degree of uncertainty in the N₂
434 values because its presence is inferred from the balance after other major gases are
435 accounted for. It is possible this assumption does not hold for such a complex site, and that
436 other gases could be present.

437

438 The three adjacent point measurements (**Figure 4**) do not register the same high levels of N₂
439 or consistently low levels of O₂. Although 10.3% vol O₂ and 8.2% vol CO₂ were recorded at
440 GG01-09, to the east of GG01-48, in August 2018 and 9.3% vol O₂ and 9.8% CO₂ at GG01-45,
441 to the west of GG01-48, in October 2019. Therefore, it seems that location GG01-48 is an
442 isolated anomaly and it should be investigated further in future surveys.

443

444 4.2.4 Gas flux

445

446 For the majority of measurements, CH₄ flux was below the limit of detection. This is
447 consistent with low CH₄ concentrations in the shallow subsurface, it suggests that there is
448 very little CH₄ actively migrating from depth.

449

450 Apart from the trends referred to in Section 4.2.2, there were no CO₂ flux measurements of
451 note. Some of the individual measurements for CO₂ flux are discussed below where they
452 help describe processes in specific locations.

453

454 4.2.5 Process-based analysis

455

456 Applying Dixon and Romanak's (2015) process-based analyses to the Glasgow Observatory
457 data indicates that the detected CO₂ was predominantly biological in origin (**Figure 14**).

458 However, there are also a number of instances where the values are just to the right of the
459 biological respiration guideline, particularly in August 2018 and October 2019 (**Figure 14a**
460 and g). Romanak et al. (2012) state that this is an indication of an external source of CO₂ or
461 oxidised methane, however, they also acknowledge that an accuracy of $\pm 2\%$ can have a
462 significant effect on the datapoints, particularly when the O₂ values are above 18%, and
463 therefore this analysis should be used in conjunction with the other two methods. The use
464 of the relationship between the N₂/O₂ ratio and CO₂ potentially dilutes the effect of higher
465 N₂, particularly if O₂ is close to atmospheric concentrations, so that only more pronounced
466 effects are displayed outside of the respiration and oxidation lines. This plot seems to
467 confirm that the CO₂ is predominantly biological in origin and does not indicate any
468 exogenous input of CO₂ or significant CO₂ dissolution (**Figure 14b, e and h**).

469

470 On the CO₂ vs O₂ plot there is only one datapoint that is clearly to the left of the methane
471 oxidation line (**Figure 14d**), indicating CO₂ dissolution (Dixon and Romanak, 2015). This
472 occurred at location GG01-48 in May 2019, discussed above (section 4.2.3 and **Figure 6**).
473 CO₂ dissolution would also be inferred based on the higher-than-atmospheric N₂ data at this
474 location (Romanak et al., 2012), see **Figure 14c, f and i**), although it would be expected to
475 see this as part of a more general trend either across several points or campaigns. However,
476 as stated, the N₂/O₂ vs CO₂ plot does not indicate CO₂ dissolution but suggests that there is
477 some oxidation of CH₄ occurring at GG01-48 as all three datapoints are either on or just over
478 the CH₄ oxidation (**Figure 14b, e and h**). It may be that both these processes are occurring at
479 this point, alternatively these explanations may not be suitable as a significant proportion of
480 the total gas is CO₂ and O₂ levels are low, particularly in August 2018 and other gases, not
481 detectable with the current instruments, may be present.

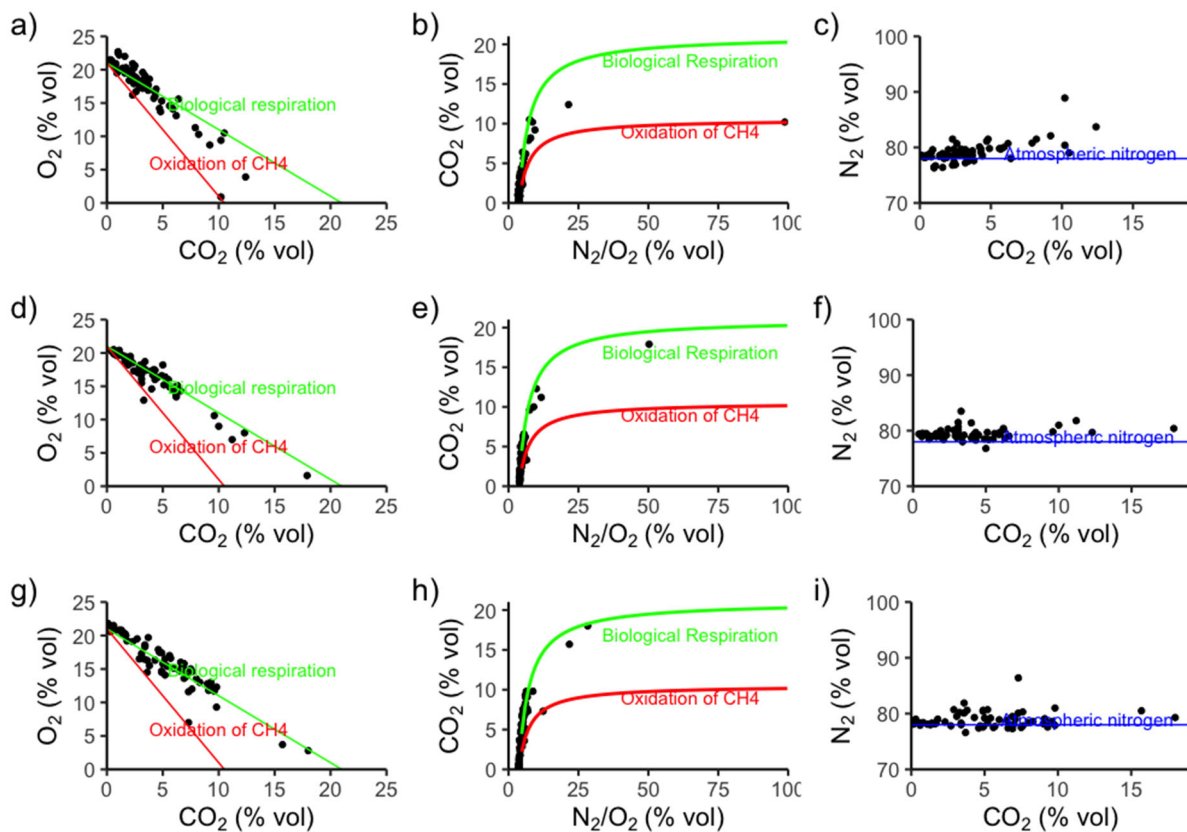


Figure 14 Comparison of the August 2018 (plots a, b) and c), May 2019 (plots d, e) and f) and October 2019 (plots g, h, i) data using the visualisation developed by Romanak et al. (2012) to characterise the sources of the ground gas. The green and red lines in plots a), b), d), e), g) and h) reflect the reaction stoichiometry relating to biological respiration and oxidation of methane, respectively. All measurements were taken using the GA 5000. See **Figure 5** for further explanation of the data visualisation.

482

483 5 Discussion

484 5.1 Background gas data – overall indications and comparisons with other sites

485

486 The data obtained for the Glasgow Observatory strongly suggest that the detected CO₂ is
 487 from biogenic sources and is consistent with other background gas data based upon land
 488 use, seasonal patterns, weather fluctuations and geography, as shown in the following
 489 sections.

490

491 5.1.1 Land use

492

493 Previous studies have looked at the role of land use. At a large-scale carbon capture project
 494 in Decatur, Illinois, Carman et al. (2014) tested the difference between CO₂ flux from bare

495 ground, where natural processes had been inhibited by the addition of herbicide, and that
496 from natural ground, where plants and microorganisms were left unfettered. They found
497 that from 2009 to 2013 the latter consistently produced, on average, more than twice the
498 levels of flux over the course of the year and the annual mean difference between the
499 treatments ranged from 2.7 to 13.7 g m⁻² d⁻¹. The summer flux levels at the Glasgow
500 Observatory are slightly higher than at Decatur but this is probably due to the increased
501 levels of vegetation at Glasgow, particularly as 70% of the data at Decatur came from bare
502 ground measurements.

503

504 The question of whether land use affects background gas measurements was also
505 considered by a study in Hobe, Denmark (Jones et al., 2014; Beaubien et al., 2015). It was
506 found that three land uses, cultivated, heath and forest, did not seem to have an impact on
507 CO₂ flux, which averaged about 15 g m⁻² d⁻¹ for May 2012 with measurements up to 75 g m⁻²
508 d⁻¹; similar to values recorded at Glasgow. There was, however, an observed difference in
509 the CO₂ concentrations, which were higher for the cultivated and heath sites, indicating that
510 overall CO₂ production was higher for these land uses. It was hypothesised that the lower
511 concentrations for the forest were due to the lower soil temperatures caused by the shade
512 of the trees. The overall mean CO₂ concentration was between 1 – 1.5% vol but the
513 cultivated site recorded concentrations of about 6% vol by the end of summer, which is
514 typical of soils in temperate zones, particularly if CO₂ production is aided by fertilisers
515 stimulating the biological processes.

516

517 In terms of a site with a more industrial history, Li et al. (2020) reported on CO₂ flux from a
518 sealed landfill site in Beijing in which they studied seasonal fluctuations in the transfer of
519 gases and identified hotspots for the escape of the gases. The CO₂ flux data at the Glasgow
520 Observatory is lower than the mean at the non-hotspot and intermediate sites, which
521 included winter data, and significantly below the hotspot measurements.

522

523 5.1.2 Seasonal pattern and weather

524

525 Seasonal CO₂ concentration and CO₂ flux measurements at the Glasgow Observatory appear
526 to have an inverse relationship (**Figure 12**). An explanation for this is that escaping CO₂,

527 creating the flux, cannot also accumulate to produce a high concentration. However, this
528 does not match observations in other studies. At Kirby Misperton and Preston New Road
529 (UK), Decatur (USA), the non-hotspots in Beijing and most markedly at Weyburn (Canada),
530 overall CO₂ levels, both as flux and ground gas concentration, were at their highest in
531 summer, followed by spring and then autumn with almost no detectable flux, if it was
532 measured, during winter (Ward et al., 2019; Carmen et al., 2014; Li et al., 2020 and
533 Beaubien et al., 2013). The CO₂ flux measurements at the Glasgow Observatory were
534 consistent with these observations, and at other UK sites (see below, Jones et al., 2014), but
535 the CO₂ concentration were not, increasing over the three seasonal campaigns.

536

537 The reason for the apparent inconsistency may be that CO₂ flux and ground gas
538 concentration are often decoupled (Beaubien et al., 2015; Jones et al., 2014). The
539 dissociation between different manifestations of CO₂ is due to biological CO₂ production at
540 different depths. Biological processes are predominantly located in the top 2.5 cm of the soil
541 and do not significantly affect accumulation at depth (Risk et al., 2002). If the pathways to
542 the surface exist, this leads to higher CO₂ flux. If they are impeded, usually by precipitation,
543 then the deeper, relatively weaker, biological CO₂ production will accumulate due to its
544 inability to escape, as seen at Kirby Misperton (Maier, 2010; Ward et al., 2019). These
545 factors must therefore be overlain on seasonal fluctuations, where it would be expected
546 that biogenic CO₂ is at its highest when there is more metabolic activity.

547

548 This more intricate situation is seen at the Glasgow Observatory when the point
549 measurements for CO₂ concentration and flux are compared (see **Figures 8** and **9**). In
550 August 2018, three out of four of the highest concentrations coincided with medium flux
551 levels. Additionally, most instances of medium to high concentration and flux are found in
552 specific localities: the north and northwest edge of Site 1, northwest and southwest edges
553 of Site 2 and southeast edge of Site 5. This indicates that total CO₂ is higher in these areas.
554 In May 2019 the higher CO₂ values are generally to the northeast side of Site 1 and there is
555 one location (GG01-29) that has both a high CO₂ concentration and flux (**Figure 6**). Overall
556 CO₂ is less pronounced at Site 2 and 5. Finally, in October 2019 the highest CO₂
557 concentrations are again in Site 1 with more modest levels at Sites 2, 3 and 5. In this
558 campaign, CO₂ flux is in the lowest category (less than 18.69 g m⁻² d⁻¹) in all but seven out of

559 the 59 measurements reflecting the difficulty CO₂ has of escaping the sub-surface, probably
560 due to the soil water content or some other physical barrier (**Figure 9**).

561

562 The Met Office weather data (2019) for Glasgow provides further context to the overall CO₂
563 flux and concentration levels at the Observatory (**Figure 15**). It shows that August 2018
564 experienced higher temperatures than May and October 2019, creating conditions for higher
565 levels of respiration. Incidentally, May 2019 experienced the most hours of sun, 193.2
566 compared with 110.6 for August 2018 and 106.4 for October 2019, and therefore may have
567 experienced the most consistent conditions for higher levels of respiration. This could
568 mitigate the potential difference in biological CO₂ production between summer and spring,
569 indicating why the difference in overall CO₂ is not larger.

570

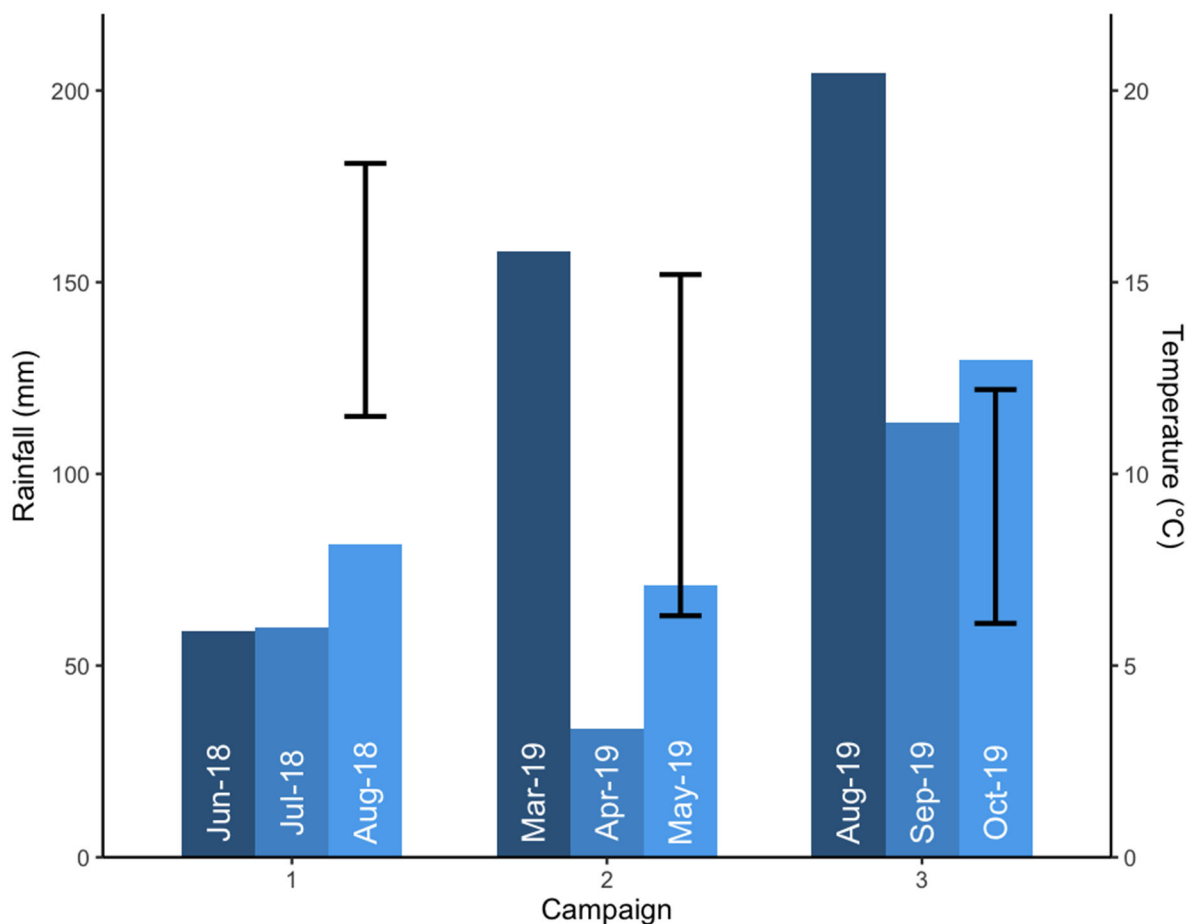


Figure 15 Rainfall data (blue bars) and temperature range (black lines) for the month of each campaign. The rainfall data for each of the two preceding months is also shown (Met Office, 2019).

571

572 It is suggested that precipitation has more impact on short-term biological CO₂ flux and
573 concentrations than soil temperature because of its wider variability (Tarakki et al., 2018;
574 Beaubien et al., 2013). This is particularly true at shallower depths, although changes in CO₂
575 concentration have also been seen at depths of 85 cm (Maier et al., 2010). This corresponds
576 to some extent with the findings of Carman et al. (2014). They observed that flux was
577 inhibited by soil moisture levels above saturation level or below wilting point and that as soil
578 moisture content reduced after heavy precipitation, flux levels significantly increased.
579 However, outside these confines Carman et al. (2014) found that soil temperature
580 correlated more closely with flux levels. This indicates that the relationship between
581 temperature, precipitation, biogenic CO₂ production and CO₂ expression is complex. For
582 instance, there is a moisture level sweet spot, where precipitation is not too high to create
583 anoxic conditions or prevent any CO₂ from escaping and not too low to prevent biological
584 activity. In Glasgow there does not seem to be a great variation in the rainfall between
585 August 2018 and May 2019 (**Figure 15**), however, October 2019 experienced significantly
586 more rainfall potentially preventing some biological activity and creating a barrier to CO₂
587 flux. In addition, there is a hysteretic effect on metabolic activity and CO₂ expression, so that
588 preceding moisture availability, coupled with temperatures, affects the abundance of living
589 matter, the soil's ability to absorb additional moisture and the ease with which gas can
590 escape. October 2019 is most impacted by previous rainfall (**Figure 15**) and, as expected, the
591 hysteretic effects on soil moisture are most apparent in the third campaign.

592

593 The difference in the seasonal weather is reflected statistically in the CO₂ data with the
594 greatest statistical difference in CO₂ flux and the only statistical difference in CO₂
595 concentration arising between the August 2018 and October 2019 campaigns. The statistical
596 difference between the CO₂ flux was smaller between the May and October 2019
597 campaigns, with the smallest difference between the August 2018 and May 2019 surveys.
598 With only one set of measurements for each season the results from the three campaigns
599 can only be suggestive of the general seasonal pattern, although they are consistent with
600 seasonal findings elsewhere, particularly when precipitation levels leading to impermeable
601 soils are taken into account (Beaubien et al., 2013; Carman et al., 2014; Jones et al., 2014
602 and Li et al., 2020). This indicates that the most likely significant factors affecting the

603 localised concentration and expression of background CO₂ is aggregate seasonal CO₂
604 production and the availability of CO₂ migration pathways.

605

606 5.1.3 Geography – other UK sites

607

608 Finally, taking into account land use and seasonality the results at the Glasgow Observatory
609 are consistent with three other UK sites: ASGARD, Nottingham; Kirby Misperton, north-east
610 England; and Preston New Road, north-west England (Jones et al., 2014; Ward et al., 2019).

611 **Figure 16** demonstrates the similarity of Glasgow’s results with the other sites; most notably
612 the consistency of the seasonal pattern of CO₂ flux measurements with Kirby Misperton.

613

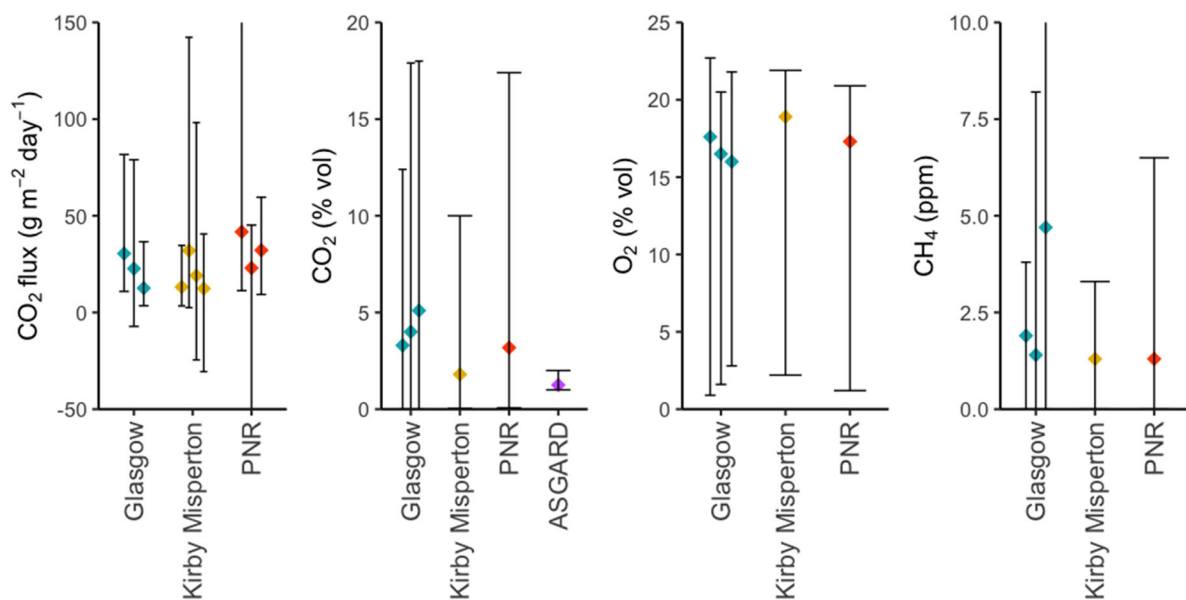


Figure 16 Comparing the three Glasgow campaigns with other UK sites. Black lines display the reported ranges and the coloured diamond indicate the mean values. CO₂ flux can be negative if the net transfer is from the atmosphere to the soil. Where the ‘t’ bars are not visible then the range is outside of the plot. Measurements at Kirby Misperton and Preston New Road (PNR) were taken over multiple campaigns (Ward et al., 2019). For Kirby Misperton they were in November 2015, June, August and October 2016 and for Preston New Road they were in August 2015, September 2016 and September 2018, however, the measurements for CO₂, O₂ and CH₄ concentrations at both Kirby Misperton and Preston New Road (PNR) sites were reported as compiled data across the surveys.

614

615 As the other three sites were all pastures, it may be expected that they would display higher
616 overall levels of CO₂ but what is most notable is that the measurements at the Glasgow
617 Observatory are unremarkable considering the complex site history. The only result that is
618 incongruous is CH₄ for the October 2019 at Glasgow, that has already been discussed. A

619 caveat to this is that there are limitations to the grid sampling method in relation to
620 detecting hot spots and more mobile surveys, such as using a quad bike or cart, would be
621 beneficial in this respect (see Barkwith et al., 2020a). However, site conditions prevented
622 the use of the ground-based, mobile, continuous sampling methods and it was necessary to
623 use a sampling grid that balanced the proximity of sampling points but still covered a
624 meaningful area.

625

626 5.2 Background gas vs Process-based approach

627

628 The above results demonstrate that background gas techniques are relevant and useful in a
629 novel setting, both in terms of their applicability to shallow geothermal investigations and at
630 sites with a complex industrial history. However, as seen, the results must be interpreted in
631 the context of factors including land use, seasonal patterns and weather; although, in
632 relation to the seasonal patterns, autumn campaigns are generally preferred to reduce the
633 biological noise (Beaubien et al., 2013; Ward et al., 2019). The background gas approach
634 provides the most comprehensive representation of the ground gas landscape as it allows
635 investigators to document a wider range of relevant gases than the four that are the focus
636 of the process-based approach. In this respect, better understanding of the occurrence and
637 causes of the less prevalent gases, such as H₂, is needed for a more thorough understanding
638 of the gas environment.

639

640 Collecting data for a background survey is a ceaseless task, particularly when set against a
641 shifting backdrop of local and global environmental changes. These surveys can be labour
642 intensive, although compared with other monitoring techniques, ground gas and flux
643 measurement costs are relatively inexpensive. As the process-based approach analyses
644 relative gas concentrations it is less affected by environmental change. It is an attractive
645 alternative as it requires fewer resources and bases its analysis on scientific principles.
646 However, each background gas survey, with its absolute measurements, assists in increasing
647 understanding of the developing global gas landscape and adds to the catalogue of
648 reference sites. This is particularly pertinent for subsurface activities below industrial sites
649 as there seems to be very few comparable published studies. The surveys also provide a
650 degree of reassurance to local communities through their visibility and by providing

651 confirmation that there is a safety net with regard to detecting any anomalies (Jenkins et al.,
652 2015).

653

654 The current work shows the process-based approach can easily be incorporated into a
655 background gas study, so that the benefits can be employed alongside a more
656 comprehensive view. However, even using the process-based tools it has been difficult to
657 characterise the anomaly at GG01-48. This is because this analysis does not provide clear
658 indications when there are two or more processes occurring simultaneously and it may be
659 that it does not account for all the processes that can affect the results. Care also needs to
660 be taken with the process-based approach as instrument accuracy or lack of sensitivity at
661 low CO₂ concentrations can affect the environmental characterisation, a common
662 occurrence during background surveys where scientists are trying to identify pre-existing
663 anomalies amongst the general background gas landscape. Instrument-based anomalies are
664 more likely to be detected in repeated background gas surveys. The process-based
665 approach seems to provide more effective results in relation to attribution where there is a
666 clear signal, but the source is uncertain. As such, it is a useful tool in relation to CO₂ storage,
667 where Dixon and Romanak (2015) assert anomalous gas should be attributed to a leakage
668 before quantification and reporting.

669

670 In some circumstances a background gas survey is required before subsurface work can
671 commence, however, it seems valuable and prudent to perform a background gas study in
672 novel situations or where there is likely to be a complex history of land use. Both novelty
673 and complexity are present at the Glasgow Observatory.

674

675 5.3 Future gas surveys

676

677 This background gas survey data will now be used as a comparison for results from future
678 gas surveys, including from an installation that will provide continuous monitoring for part
679 of the site. The continuous monitoring will include ground temperature measurements,
680 which have currently been inferred from local weather reports, allowing for a more accurate
681 understanding of the conditions for biological activity. If a wide range of variables continues
682 to be monitored, it is likely that one of the elements will display an unusual result and so it

683 is sensible to refine the array of variables measured to the ones that are most likely to
684 identify consequences from the investigations into low enthalpy heat from the mine
685 workings. In this respect it may be possible to adapt the signal to noise ratio (SNR)
686 technique employed to make the measurement, monitoring and verification (MMV) of CO₂
687 storage more robust (Risk et al., 2013; Nickerson and Risk, 2013 and Risk et al., 2015). In this
688 setting the technique is used when the signature of the injected gas is known, however, it
689 can be adapted so that the post-operational measurements can be compared with
690 background gas measurements. From the results at the Observatory, it is apparent that the
691 most consistently similar means and distribution are the N₂ measurements, potentially
692 providing the clearest signal to noise ratio, although issues may arise because they are proxy
693 measurements.

694

695 6 Conclusions

696

697 Background ground gas and gas flux surveys were employed in three campaigns, undertaken
698 in three different seasons, across four sites as part of establishing an environmental
699 baseline at a geenergy observatory for mine water heat in Glasgow, UK. The research
700 infrastructure is located at a site with complex former land use but as there was no
701 statistical difference in the results between the sites, each campaign was treated as a single
702 sample.

703

704 Overall, the results showed some seasonal fluctuations but background gas characteristics
705 were consistent with a biogenic origin and were typical when compared with other sites
706 taking into account land use, seasonal fluctuations and geography. Considering the historical
707 industrial uses of the site the results were unremarkable with only one anomaly for CH₄,
708 some sample points of interest for future campaigns, particularly GG01-48, and several
709 elevated measurements of H₂, albeit well below the explosive limit. This highlighted the lack
710 of published studies about H₂ in the shallow subsurface at former industrial sites that would
711 improve our understanding of potential H₂ sources detected in this work. There was some
712 evidence of oxidation of CH₄, particularly at Site 1, but low values of mine gases, CH₄, H₂S
713 and H₂, indicate it was unlikely that the mine workings were a significant source of CH₄.

714

715 In addition to contributing to the catalogue of background environmental evidence,
716 particularly of sites with substantial anthropogenic land-use, the survey results also
717 illuminate the benefits and short-comings of the baseline and process-based approaches.
718 Although the process-based method did assist in characterising the gas origin, and indicated
719 that the CO₂ was biogenic, it did not replace the benefits of a background gas surveys, which
720 enabled a more detailed picture. There were limitations with the process-based approach in
721 relation to determining the origin of gas when there was not a clear signal and when there
722 were potentially more than one process occurring simultaneously. The techniques used in
723 background gas surveys are relevant for the exploration of low-enthalpy, shallow
724 geothermal energy and it seems prudent to utilise them in novel situations, either due to
725 the innovative technologies involved or the complexity of the subsurface environment.

726

727 Using an adaption of the SNR technique in future post-operational analysis may assist in
728 distinguishing true anomalies from the normal background variations in data.

729

730 7 Data Availability

731

732 Further details about the data release for the three campaigns are contained in Barkwith et
733 al. (2020b) and the data can be found at National Geoscience Data Centre (2021) or using
734 <https://doi.org/10.5285/2f98e806-1713-4ac9-8c91-bbf8e1a5ee7d>. All data relating to the
735 UKGEOS observatories can be found at <https://ukgeos.ac.uk>.

736

737 8 Acknowledgements

738

739 The authors would like to acknowledge the input of Alison Monaghan for providing valuable
740 contributions to improving the manuscript. We also wish to thank the reviewers for their
741 constructive comments.

742

743 **9 Funding Sources**

744

745 The UK Geenergy Observatories are funded by the Natural Environment Research Council
 746 (NERC) supported by UK Government’s Department for Business, Energy & Industrial
 747 Strategy (BEIS).

748 **10 Appendix A – Instrument specifications**

749

Instrument	Gas	Measurement range	Accuracy
GA 5000	CH ₄ concentration	0-100%	0-70% : ±0.5% (vol), 70-100% : ±1.5% (vol)
	CO ₂ concentration	0-100%	0-60% : ±0.5% (vol), 60-100% : ±1.5% (vol)
	O ₂ concentration	0-25%	0-25% : ±1.0% (vol)
	H ₂ S concentration	0-1,000 ppm	±2.0% FS
	H ₂ concentration	0-1,000 ppm	±2.5% FS
Laser One	CH ₄ concentration	1-10,000 ppm	+/-0.7ppm for [1: 10ppm] +/-10% relative up to 10,000
Li-COR® model LI820 analyser	CO ₂ flux	0 – 20000 ppm with 5 cm optical bench	4% of reading with 5 cm bench

750

751 **11 References**

752

753 Athresh, A.P, Al-Habaibeh, A. and Parker, K. (2015) *Innovative approach for heating of*
 754 *buildings using water from a flooded coal mine through an open loop based single shaft*
 755 *GSHP system*, Energy Procedia, 75, 1221–1228 [online]. Available at
 756 <https://doi.org/10.1016/j.egypro.2015.07.162>.

757

758 Appleton, J.D. (2011) *User Guide for the BGS Methane and carbon dioxide from natural*
 759 *sources and coal mining dataset for Great Britain* [contributor/editor K. Royce]. British
 760 Geological Survey Open Report OR/11/054 [online]. Available at
 761 <http://pubs.bgs.ac.uk/publications.html?pubID=OR11054>.

762

763 Ball, T. K., Peachey, D. and Vickers, B P. (1992) *Geochemical Methods Handbook*, Volume 3:
 764 *Soil gas techniques for use in geochemical surveys overseas*. British Geological Survey
 765 Research Report SI/92/3 (Keyworth, Nottingham).

766

767 Banks, D., Athresh, A., Al-Habaibeh, A. and Burnside, N. (2017) *Water from abandoned*
 768 *mines as a heat source: practical experiences of open and closed-loop strategies*, *United*
 769 *Kingdom*, Sustainable Water Resources Management, 5, 29-50 [online]. Available at
 770 <https://doi.org/10.1007/s40899-017-0094-7>.

771

772 Barkwith, A., Beaubien, S. E., Barlow, T., Kirk, K., Lister, T. R., Tartarello, M. C., and Taylor, H.
773 (2020a) Using near-surface atmospheric measurements as a proxy for quantifying field-scale
774 soil gas flux, *Geosci Instrum* [online]. Available at <https://doi.org/10.5194/gi-2020-8>.
775

776 Barkwith, A.K.A.P., Lister, T.R., Taylor-Curran, H., Hannis, S., Shorter, K., Walker-Verkuil, K.,
777 Kirk, K., Smith, D. and Monaghan, A. (2020b) *Data Release Notes: UK Geoenery*
778 *Observatories Glasgow Geothermal Energy Research Field Site (GGERFS) Ground Gas, 2018*
779 *and 2019 Surveys*. British Geological Survey Open Report OR/20/037 (Keyworth,
780 Nottingham).
781

782 Beaubien, S.E., Jones, D.G., Gal, F., Barkwith, A.K.A.P, Braibant, G., Baubron, J.-C., Ciotoli, G.,
783 Graziani, S., Lister, T.R., Lombardi, K., Michel, K., Quattrocchi, F. and Strutt, M.H. (2013)
784 *Monitoring of near-surface gas geochemistry at the Weyburn, Canada, CO₂-EOR site, 2001 –*
785 *2011* *International Journal of Greenhouse Gas Control*, 16S (2013), S236–S262.
786

787 Beaubien, S.E., Ruggiero, L., Annunziatellis, A., Bigi, S., Ciotoli, G., Deiana, P., Graziani, S.,
788 Lombardi, S. and Tartarello, M.C. (2015) *The Importance of Baseline Surveys of Near-Surface*
789 *Gas Geochemistry for CCS Monitoring, as Shown from Onshore Case Studies in Northern and*
790 *Southern Europe* *Oil Gas Sci. Technol* 70, 4, 615-633.
791

792 BEIS (2019) *Energy Consumption in the UK (ECUK)* [online]. Department for Business, Energy
793 and Industrial strategy. Available at
794 [https://assets.publishing.service.gov.uk/government/uploads/system/uploads/attachment](https://assets.publishing.service.gov.uk/government/uploads/system/uploads/attachment_data/file/820843/Energy_Consumption_in_the_UK_ECUK_MASTER_COPY.pdf)
795 [data/file/820843/Energy Consumption in the UK ECUK MASTER COPY.pdf](https://assets.publishing.service.gov.uk/government/uploads/system/uploads/attachment_data/file/820843/Energy_Consumption_in_the_UK_ECUK_MASTER_COPY.pdf).
796

797 Blackford J., Stahl H., Bull J., Bergès B., Cevatoglu M., Lichtschlag A., Connelly D., James R.,
798 Kita J., Long D., Naylor M., Shitashima K., Smith D., Taylor P., Wright I., Akhurst M., Chen B.,
799 Gernon T., Hauton C., Hayashi M., Kaieda H., Leighton T., Sato T., Sayer M., Suzumura M.,
800 Tait K., Vardy M., White P., Widdicombe S. (2014) *Detection and impacts of leakage from*
801 *sub-seafloor deep geological carbon dioxide storage*, *Nature Climate Change*, 2014 vol: 4
802 (11) pp: 1011-1016.
803

804 Burkin, J. and Kearsley, T. (2019) *Model metadata report for Glasgow Geothermal Energy*
805 *Research Field Site bedrock model*. British Geological Survey Open Report, OR/18/053. 18pp.
806

807 Cardellini, C., Chiodini, G., Frondini, F., Granieri, D., Lewicki, J., and Peruzzi, L. (2003)
808 *Accumulation chamber measurements of methane fluxes: application to volcanic-*
809 *geothermal areas and landfills*. *Applied Geochemistry*, Vol. 18, 45-54.
810

811 Carman, C. H., Locke II, R. A. and Blakley, C. S. (2014) *Update on Soil CO₂ Flux Monitoring at*
812 *the Illinois Basin – Decatur Project*, *USA Energy Procedia* 63 (2014) 3869 – 3880
813 doi:10.1016/j.egypro.2014.11.417.
814

815 Castaldi S. (2000) *Responses of nitrous oxide, dinitrogen and carbon dioxide production and*
816 *oxygen consumption to temperature in forest and agricultural light-textured soils*
817 *determined by model experiment*, *Biology and Fertility of Soils* 32, 1, 67-72,
818 doi:10.1007/s003740000218.

819
820 CCC (2019) *Net Zero – The UK’s contribution to stopping global warming* [online]. Available
821 at [https://www.theccc.org.uk/publication/net-zero-the-uks-contribution-to-stopping-](https://www.theccc.org.uk/publication/net-zero-the-uks-contribution-to-stopping-global-warming/)
822 [global-warming/](https://www.theccc.org.uk/publication/net-zero-the-uks-contribution-to-stopping-global-warming/).
823
824 Chapin, F.S., III, Matson, P.M. and Vitousek, P.M. (2012) *Principles of Terrestrial Ecosystem*
825 *Ecology* (2nd ed). London, Springer.
826
827 Coal Authority (2021) *Geothermal energy from abandoned coal mines* [online]. Available at
828 <https://www2.groundstability.com/geothermal-energy-from-abandoned-coal-mines/>.
829
830 DECC (2013) *The Unconventional Hydrocarbon Resources of Britain’s Onshore Basins -*
831 *Coalbed Methane (CBM)* [online]. Available at
832 https://www.ogauthority.co.uk/media/1694/promote_uk_cbm_2012.pdf.
833
834 Dixon T. and Romanak K. (2015) *Improving monitoring protocols for CO2 geological storage*
835 *with technical advances in CO2 attribution monitoring* *International Journal of Greenhouse*
836 *Gas Control* 2015 vol: 41 pp: 29-40.
837
838 Farr, G., Busby, J., Wyatt, L., Crooks, J., Schofield, D.I. and Holden, A. (2020) *The temperature*
839 *of Britain’s coalfields*, *Quarterly Journal of Engineering Geology and Hydrogeology*,
840 :qjgeh2020-109 [online]. Available at <https://doi.org/10.1144/qjgeh2020-109>.
841
842 Flude, S., Györe, D., Stuart, F., Zurakowska, M., Boyce, A., Haszeldine, R., Chalaturnyk, R. and
843 Gilfillan S. (2017) *The inherent tracer fingerprint of captured CO₂*, *International Journal of*
844 *Greenhouse Gas Control*, 2017 vol: 65 (July) pp: 40-54.
845
846 Fordyce, F.M., Shorter, K.M., Vane, C. H., Gowing, C. J. B., Hamilton, E. M., Kim, A. W.,
847 Everett, P. A., Marchant, B. P., and Lister, T. R. (2020) *UK Geoenergy Observatories, Glasgow*
848 *Environmental Baseline Soil Chemistry Dataset*. British Geological Survey Open Report,
849 OR/19/062. 77pp.
850
851 Geotech (n.d.) *Portable gas analyser: Landfill and contaminated land* [Online]. Available at
852 <https://www.qedenv.com/products/ga-5000/>.
853
854 Glass, G.V., Peckham, P.D. and Sanders, J.R. (1972) *Consequences of Failure to Meet*
855 *Assumptions Underlying the Fixed Effects Analyses of Variance and Covariance*, *Review of*
856 *Educational Research* vol 42, 3, pp 237-288 [online]. Available at
857 <https://doi.org/10.3102/00346543042003237>.
858
859 IPCC (2005) *Carbon Capture and Storage* Prepared by Working Group III of the
860 Intergovernmental Panel on Climate Change [(Edited by) Bert Metz, Ogunlade Davidson,
861 Heleen de Coninck, Manuela Loos and Leo Meyer] Cambridge University Press, UK. pp 431
862 [online]. Available at <https://www.ipcc.ch/report/carbon-dioxide-capture-and-storage/>.
863

864 IPCC (2006) *IPCC Carbon Dioxide Transport, Injection and Geological Storage* in Guidelines
865 for National Greenhouse Gas Inventories, Vol.2, Energy Ch 5 [online]. Available at
866 <https://www.ipcc-nggip.iges.or.jp/public/2006gl/vol2.html>.
867

868 IPCC (2014) *Climate Change 2014: Synthesis Report. Contribution of Working Groups I, II and*
869 *III to the Fifth Assessment Report of the Intergovernmental Panel on Climate Change* [Core
870 Writing Team, R.K. Pachauri and L.A. Meyer (eds.)] [online]. Available at
871 https://www.ipcc.ch/site/assets/uploads/2018/02/SYR_AR5_FINAL_full.pdf.
872

873 IPCC (2018) *Summary for Policymakers. In: Global Warming of 1.5°C. An IPCC Special Report*
874 *on the impacts of global warming of 1.5°C above pre-industrial levels and related global*
875 *greenhouse gas emission pathways, in the context of strengthening the global response to*
876 *the threat of climate change, sustainable development, and efforts to eradicate poverty*
877 [Masson-Delmotte, V., P. Zhai, H.-O. Pörtner, D. Roberts, J. Skea, P.R. Shukla, A. Pirani, W.
878 Moufouma-Okia, C. Péan, R. Pidcock, S. Connors, J.B.R. Matthews, Y. Chen, X. Zhou, M.I.
879 Gomis, E. Lonnoy, T. Maycock, M. Tignor, and T. Waterfield (eds.)]. World Meteorological
880 Organization, Geneva, Switzerland, 32 pp. Available at
881 <https://www.ipcc.ch/sr15/chapter/spm/>.
882

883 Jenkins, C., Chadwick, A. and Hovorka, S.D. (2015) *The state of the art in monitoring and*
884 *verification—Ten years on*, International Journal of Greenhouse Gas Control 40 (2015) 312–
885 349.
886

887 Jenkins, C. (2020) *The State of the Art in Monitoring and Verification: an update five years*
888 *on*, International Journal of Greenhouse Gas Control 100 (2020) 103118.
889

890 Jones, N.S., Holloway, S., Creedy, D.P., Garner, K., Smith, N.J.P., Browne, M.A.E. and Durucan
891 S. (2004) *UK Coal Resource for New Exploitation Technologies. Final Report*. British
892 Geological Survey Commissioned Report CR/04/015N [online]. Available at
893 <http://nora.nerc.ac.uk/id/eprint/509526/1/CR04015N.pdf>.
894

895 Jones, D.G., Beaubien, S.E., Barlow, T.S., Barkwith, A.K.A.P., Hannis, S.D., Lister, T.R., Strutt,
896 M.H., Bellomo, T., Annunziatellis, A., Graziani, S., Lombardi, S., Ruggiero, L., Braibant, G., Gal,
897 F., Joubin, F. and Michel, K. (2014) *Baseline variability in onshore near surface gases and*
898 *implications for monitoring at CO₂ storage sites* Energy Procedia 63 (2014) 4155 – 4162
899 doi:10.1016/j.egypro.2014.11.447.
900

901 Jones, D.G., Beaubien, S.E., Blackford, J.C., Foekema, E.M., Lions, J., De Vittor, C., West, J.M.,
902 Widdicombe, S., Hauton, C., Queirós, A.M. (2015) *Developments since 2005 in*
903 *understanding potential environmental impacts of CO₂ leakage from geological storage*,
904 International Journal of Greenhouse Gas Control 40 (2015) 350–377.
905

906 Li-COR (n.d.) *Li-COR 820 CO₂ analyser* [online]. Available at
907 <https://www.licor.com/documents/ww4sm0xupfr051ti3amn>.
908

909 Li, H., Meng, B., Yue, B., Gao, Q., Ma, Z., Zhang, W., Li, T. and Yu, L. (2020) *Seasonal CH₄ and*
910 *CO₂ effluxes in a final covered landfill site in Beijing, China* *Science of the Total Environment*
911 725 (2020) 138355 <https://doi.org/10.1016/j.scitotenv.2020.138355>.
912

913 Maier, M., Schack-Kirchner, H., Hildebrand, E.E., Holst, J. (2010) *Pore-space CO₂ dynamics in*
914 *a deep, well-aerated soil*. *European Journal of Soil Science* 61, 877–887.
915

916 Met Office (2019) *Historic Station Data: Paisley* [online]. Available at
917 <https://www.metoffice.gov.uk/pub/data/weather/uk/climate/stationdata/paisleydata.txt>.
918

919 Monaghan A. A. O., Dochartaigh B., Fordyce F., Loveless S., Entwisle D., Quinn M., Smith K.,
920 Ellen R., Arkley S., Kearsey T., Campbell S. D. G., Fellgett M., Mosca I. (2017) *UKGEOS -*
921 *Glasgow Geothermal Energy Research Field Site (GGERFS): Initial summary of the geological*
922 *platform*, British Geological Survey Open Report, OR/17/006. 205pp [online]. Available at
923 <http://nora.nerc.ac.uk/id/eprint/518636/>.
924

925 Monaghan, A.A., Starcher, V., Dochartaigh, B Ó, Shorter, K., Burkin, J. (2019a) *UK Geoenergy*
926 *Observatories: Glasgow Geothermal Energy Research Field Site: SCIENCE INFRASTRUCTURE*
927 *VERSION 2* British Geological Survey Open Report, OR/19/032 [online]. Available at
928 <http://nora.nerc.ac.uk/id/eprint/522814/>.
929

930 Monaghan, A. (2019b) *How things change — a UK Geoenergy Observatory in Glasgow*, *The*
931 *Edinburgh Geologist* (65), 20-25.
932

933 Monaghan A. A., Starcher V., Barron, H. (2020) *UK Geoenergy Observatories Glasgow:*
934 *express data release, mine water and environmental baseline monitoring boreholes at*
935 *Cuningar Loop (updated June 2020)* British Geological Survey Open Report, OR/20/02. 17pp.
936 Available at http://nora.nerc.ac.uk/id/eprint/526889/1/OR20002_updated.pdf
937

938 Moore, T.A. (2012) *Coalbed methane: A review*, *International Journal of Coal Geology* 101
939 (2012) 36–81.
940

941 National Geoscience Data Centre (2021) *UKGEOS Glasgow Geothermal Ground Gas, 2018*
942 *and 2019 Surveys*, Item ID 138705 [online]. Available at [https://www.bgs.ac.uk/geological-](https://www.bgs.ac.uk/geological-data/national-geoscience-data-centre/)
943 [data/national-geoscience-data-centre/](https://www.bgs.ac.uk/geological-data/national-geoscience-data-centre/).
944

945 Nickerson, N. and Risk, D. (2013) *Using subsurface CO₂ concentrations and isotopologues to*
946 *identify CO₂ seepage from CCS/CO₂-EOR sites: A signal-to-noise based analysis*,
947 *International Journal of Greenhouse Gas Control* 14 (2013) 239–246.
948

949 Pearce, J., Jones, D., Blackford, J., Beaubien, S., Foekema, E., Gemeni, V., Kirk, K., Lions, J.,
950 Metcalfe, R., Moni, C., Smith, K., Stevens, M., West, J., Ziogou, F. (2014) *A guide for*
951 *assessing the potential impacts on ecosystems of leakage from CO₂ storage sites*, *Energy*
952 *Procedia* 63 (2014) 3242 – 3252.
953

954 QED (2020) *Laser One* [Online]. Available at <https://www.qedenv.com/products/laser-one/>.
955

956 Ramboll (2018) *UK Geoenergy Observatories: Glasgow Geothermal Energy Research Field*
957 *Site Environmental Report*. GGERFS planning applications for Glasgow City Council [online].
958 Available at [https://publicaccess.glasgow.gov.uk/online-](https://publicaccess.glasgow.gov.uk/online-applications/applicationDetails.do?activeTab=documents&keyVal=P70V2DEXFH600)
959 [applications/applicationDetails.do?activeTab=documents&keyVal=P70V2DEXFH600](https://publicaccess.glasgow.gov.uk/online-applications/applicationDetails.do?activeTab=documents&keyVal=P70V2DEXFH600).
960

961 Risk, D., Kellman, L., and Beltrami, H. (2002) *Soil CO₂ production and surface flux at four*
962 *climate observatories in eastern Canada* Global Biogeochemical Cycles, Vol. 16, No. 4, 1122,
963 doi:10.1029/2001GB001831, 2002.
964

965 Risk, D., McArthur, G., Nickerson, N., Phillips, C., Harta, C., Egana, J. and Lavoiea, M. (2013)
966 *Bulk and isotopic characterization of biogenic CO₂ sources and variability in the Weyburn*
967 *injection area* International Journal of Greenhouse Gas Control 16S (2013) S263–S275.
968

969 Risk, D., Lavoie, M. and Nickerson, N. (2015) *Using the Kerr investigations at Weyburn to*
970 *screen geochemical tracers for near-surface detection and attribution of leakage at CCS/EOR*
971 *sites*, International Journal of Greenhouse Gas Control, 2015 vol: 35 pp: 13-17.
972

973 Romanak, K. D., Bennett, P. C., Yang, C., and Hovorka, S.D. (2012) *Process-based approach to*
974 *CO₂ leakage detection by vadose zone gas monitoring at geologic CO₂ storage sites*,
975 Geophysical Research Letters, Vol 39, L15405, doi:10.1029/2012GL052426, 2012.
976

977 Romanak, K., Sherk, G. W., Hovorka, S. and Yang, C. (2013) *Assessment of alleged CO₂*
978 *leakage at the Kerr farm using a simple process-based soil gas technique: Implications for*
979 *carbon capture, utilization, and storage (CCUS) monitoring* Energy Procedia 37 (2013) 4242 –
980 4248.
981

982 Tarakki, N., Risk, D., Spafford, L. and Fougère C. (2018) *A meta-analysis of the surface soil*
983 *gas measurement monitoring and verification (MMV) program at the Aquistore project*,
984 International Journal of Greenhouse Gas Control, Volume 75, August 2018, Pages 189-197.
985

986 UKGEOS (2021) *UK Geoenergy Observatories* [online]. Available at
987 <https://www.ukgeos.ac.uk>.
988

989 Ward, R.S., Smedley, P.L., Allen, G., Baptie, B.J., Barkwith, A.K.A.P., Bateson, I., Bell, R.A.,
990 Bowes, M., Coleman, M., Cremen, G., Daraktchieva, Z., Gong, M., Howarth, C.H., Fisher, R.,
991 Hawthorn, D., Jones, D.G., Jordan, C., Lanoisellé, M., Lewis, A.C., Lister, T.R., Lowry, D.,
992 Lockett, R., Mallin-Martin, D., Marchant, B.P., Milne, C.J., Novellino, A., Pitt, J., Purvis, R.M.,
993 Rivett, M.O., Shaw, J., Taylor-Curran, H., Wasikiewicz, J.M., Werner, M. and Wilde, S. (2019)
994 *Environmental Monitoring - Phase 4 Final Report (April 2018 - March 2019)* British
995 Geological Survey Open Report, OR/19/044. 225 pp.
996

997 Wilson, S., Card, G. and Haines, S. (2010) *Ground Gas Handbook* Dunbeath GBR, Whittles
998 Publishing.
999

1000 Young, B. and Lawrence, D. (2001) *A Breath of Fresh Air? The unseen dangers of mine gas*
1001 *Earthwise* 17 (2001), 16-17.
1002

1003 Zgonnik, V. (2020) *The occurrence and geoscience of natural hydrogen: A comprehensive*
1004 *review* Earth-Science Reviews 203 (2020) 103140
1005 <https://doi.org/10.1016/j.earscirev.2020.103140>.
1006
1007 Zhang, L., Guo, Z., Sano, Y., Zhang, M., Sun, Y., Cheng, Z., and Yang, T.F. (2017) *Flux and*
1008 *genesis of CO₂ degassing from volcanic-geothermal fields of Gulu-Yadong rift in the Lhasa*
1009 *terrane, South Tibet: Constraints on characteristics of deep carbon cycle in the India-Asia*
1010 *continent subduction zone*. Journal of Asian Earth Sciences, Vol. 149, 110-123.
1011